

1 **Evolution of the firn pack of Kaskawulsh Glacier, Yukon: meltwater**
2 **effects, densification, and the development of a perennial firn aquifer**

Shawn Marshall 12/28/2020 10:25 AM
Deleted: warming, ...nd the creation ... [1]

3
4 Naomi Ochwat¹, Shawn Marshall^{1,2}, Brian Moorman¹, Alison Criscitiello,³ Luke Copland⁴

5 ¹Department of Geography, University of Calgary, Calgary, Alberta, T2N 1N4, Canada

6 ²Environment and Climate Change Canada, Gatineau, Quebec, K1A 0H3, Canada

7 ³Department of Earth and Atmospheric Sciences, University of Alberta, Edmonton, T6G 2R3, Canada

8 ⁴Department of Geography, Environment and Geomatics, University of Ottawa, Ottawa, Ontario K1N 6N5, Canada

9
10 *Correspondence to:* Naomi Ochwat (naomi.ochwat@ucalgary.ca)

11
12 **Abstract.** In spring 2018, two firn cores (21 m and 36 m in length) were extracted from the accumulation zone of
13 Kaskawulsh Glacier, St. Elias Mountains, Yukon. The cores were analyzed for ice layer stratigraphy and density, and
14 compared against historical measurements made in 1964 and 2006. Deep meltwater percolation and refreezing events were
15 evident in the cores, with a total ice content of 2.33 ± 0.26 m in the 36-m core and liquid water discovered below a depth of
16 34.5 m. Together with the observed ice content, surface energy balance and firn modelling indicate that Kaskawulsh Glacier
17 firn retained about 73% of its meltwater in the years 2005-2017. For an average surface ablation of 0.38 m w.e. yr⁻¹ over this
18 period, an estimated 0.17 m w.e. yr⁻¹ refroze in the firn, 0.065 m w.e. yr⁻¹ was retained as liquid water, and 0.105 m w.e. yr⁻¹
19 drained or ran off. The refrozen meltwater is associated with a surface lowering of 0.73 ± 0.23 m between 2005 and 2017
20 (i.e., surface drawdown that has no associated mass loss). The firn has become denser and more ice-rich since the 1960s, and
21 contains a perennial firn aquifer (PFA), which may have developed over the past decade. This illustrates how firn may be
22 evolving in response to climate change in the St. Elias Mountains, provides firn density information required for geodetic
23 mass balance calculations, and is the first documented PFA in the Yukon-Alaska region.

Shawn Marshall 1/28/2021 5:48 PM
Deleted: Meltwater ...eep meltwater perco... [2]

Shawn Marshall 1/28/2021 10:21 AM
Formatted

Shawn Marshall 12/28/2020 10:27 AM
Deleted: ; (ii)...has become warmer, ... [4]

59 With the increasing effects of climate change and the need for understanding glacier and ice sheet melt rates, geodetic
 60 methods are useful for indirect measurements of mass balance (Cogley, 2009). Based on repeat altimetry, geodetic
 61 approaches to mass balance monitoring rely on several assumptions. Estimates must be made of the density of snow, firn,
 62 and ice at the sampling location, with the additional assumption that these densities remain unchanged between the two
 63 measurement dates. However, over multi-annual timescales in a warming climate this may not be true (Moholdt et al.,
 64 2010b). Meltwater percolation and refreezing can significantly change the firn density profile and mean density of the
 65 accumulation zone of a glacier (Gascon et al., 2013), and can introduce large uncertainties when using geodetic techniques to
 66 determine glacier mass balance if they are not properly accounted for. For example, Moholdt et al. (2010a) determined the
 67 geodetic mass balance of Svalbard glaciers to be $-4.3 \pm 1.4 \text{ Gt yr}^{-1}$, based on ICESat laser altimetry, with the large
 68 uncertainty attributed to limited knowledge of the snow and firn density and their spatial and temporal variability. By
 69 altering the density and causing surface lowering, meltwater percolation, refreezing, and liquid water storage all complicate
 70 the interpretation of geodetic mass balance data.

71
 72 Warming firn can result in increased meltwater production and altered firn densification processes. Initially, melt can round
 73 the snow grains and increase the snowpack density. ~~Meltwater can percolate into the firn and refreeze as ice layers or lenses.~~
 74 On glaciers with medium to high surface melt, and high annual snow accumulation, meltwater that percolates below the
 75 winter cold layer often will not refreeze, and may thus form a perennial firn aquifer (PFA) if this water cannot effectively
 76 drain through crevasses or moulins (Kuipers Munneke, et al., 2014). These internal accumulation processes can significantly
 77 increase the firn density, and once ice layers or PFAs form they affect how meltwater percolates through the firn pack
 78 (Gascon et al., 2013). Due to the spatial heterogeneity of meltwater retention, percolation, and refreezing processes, there are
 79 still many gaps in knowledge of how to model these processes and subsequently estimate firn density in areas where these
 80 processes occur (van As et al., 2016).

81
 82 Meltwater retention in firn is also important for estimating glacial runoff contributions to sea level rise. Numerous recent
 83 studies have investigated meltwater refreezing processes in northern locations such as southern Greenland (Humphrey et al.,
 84 2012; Harper et al., 2012; De La Peña et al., 2015; MacFerrin et al., 2019), Canadian Arctic Archipelago (Noël et al. 2018,
 85 Zdanowicz et al., 2012; Bezeau et al., 2013; Gascon et al., 2013), and Svalbard (Noël et al. 2020, Van Pelt et al., 2019,
 86 Christianson et al., 2015). In many locations, short term increases in surface melt rates may not result in proportional
 87 increases in surface runoff due to percolation and refreezing of meltwater in the firn pack (e.g., Harper et al., 2012; Koenig
 88 et al., 2014; MacFerrin et al., 2019). However, in the long term this may lead to expansion of low-permeability ice layers,
 89 causing run-off to increase and expediting the movement of water from glaciers to the ocean (MacFerrin et al., 2019).

Naomi Ochwat 1/29/2021 11:40 AM

Deleted: If the surface continues to melt, the

Naomi Ochwat 1/29/2021 11:40 AM

Deleted: m

Naomi Ochwat 1/17/2021 8:52 PM

Deleted: Munneke

Naomi Ochwat 1/28/2021 10:20 PM

Deleted: firn aquifer

94 | [Machguth et al., 2016](#)). Current knowledge of these processes is limited for mountain glaciers in other regions, although this
95 | information is required for improved estimates and models of glacier mass balance and associated sea-level rise.

96 |
97 | In this study two firn cores were retrieved in spring 2018 on Kaskawulsh Glacier, [St. Elias Mountains](#), Yukon, and analyzed
98 | for density and the effects of meltwater percolation and refreezing. Comparisons of these measurements with firn density
99 | profiles and temperatures collected at a nearby site in 1964 and 2006 enable us to: (i) Quantify contemporary firn
100 | characteristics and densification processes; (ii) Determine how the physical properties of the firn pack have changed over the
101 | past ~50 years; and (iii) Assess the likelihood of a widespread [PFA on the upper Kaskawulsh Glacier](#).

102 2 Study area

103 | The St. Elias Mountains are located in the southwest corner of Yukon Territory, Canada, and contain many peaks higher than
104 | 3000 m, including the highest mountain in Canada, Mount Logan, at 5959 m a.s.l. (Figure 1). The St. Elias is home to the
105 | largest icefield outside of the polar regions, with an area of ~46,000 km² (Berthier et al., 2010). [Measurements presented
106 | here are focused on the upper accumulation zone of Kaskawulsh Glacier \(Figure 1\), which is part of an extensive \(~63 km²\)
107 | snowfield at an elevation of 2500-2700 m a.s.l. This plateau region has subtle topographic variations and includes the
108 | drainage divide between the Kaskawulsh and Hubbard Glaciers.](#)

109 |
110 | Kaskawulsh Glacier is a large valley glacier located on the eastern side of the St. Elias Mountains within the Donjek Range,
111 | and is approximately 70 km long and 3-4 km wide. Our 2018 drill site was located on the upper north arm of the glacier in
112 | the accumulation zone (60.78°N, 139.63°W), at an elevation of 2640 m a.s.l. Based on satellite imagery, Foy et al. (2011)
113 | estimated an average equilibrium line altitude (ELA) for the glacier of 1958 m a.s.l. for the period 1977-2007, while Young
114 | et al. (2020) provided a mean ELA of 2261 ±151 m a.s.l. for the years 2013-2019. Our core site [is thus well above the ELA,
115 | and has remained within the main accumulation area of the glacier. Mean annual and summer \(JJA\) air temperatures from
116 | 1979-2019 were -10.7°C and -2.5°C, respectively, based on bias-adjusted ERA5 climate reanalyses \(Hersbach et al., 2020\).](#)
117 | The main melt season occurs from June through August. [Over the period 1979-2016, Williamson et al. \(2020\) reported that
118 | the St. Elias Icefield air temperature warmed at an average rate of 0.19°C decade⁻¹ at an elevation of 2000-2500 m a.s.l.,
119 | rising to 0.28°C decade⁻¹ at an elevation of 5500-6000 m a.s.l.](#)

120 |
121 | Previous studies of Kaskawulsh Glacier have included an analysis of volume change over time based on comparisons of
122 | satellite imagery and digital elevation models (Foy et al., 2011; Young et al., 2020). Several reports in the 1960s documented
123 | various glaciological characteristics and processes occurring in the St. Elias Icefields, as part of the Icefield Ranges Research
124 | Project ([IRRP](#)) (Wood, 1963; Grew and Mellor, 1966; Marcus and Ragle, 1970). [Firn density and temperature measurements
125 | to 15-m depth were made during this period at site IRRP A, near the Kaskawulsh-Hubbard divide and about 5 km from our](#)

Naomi Ochwat 1/28/2021 10:20 PM

Deleted: perennial firn aquifer

Naomi Ochwat 1/28/2021 10:20 PM

Deleted: (PFA)

Shawn Marshall 1/7/2021 8:14 AM

Deleted: across the St. Elias Icefield

Shawn Marshall 1/7/2021 8:19 AM

Deleted: Measurements are focused on the upper accumulation zone of Kaskawulsh Glacier (Figure 1), near the drainage divide with Hubbard Glacier.

Naomi Ochwat 1/27/2021 9:58 PM

Deleted: ***

Shawn Marshall 1/28/2021 10:29 AM

Formatted: Not Highlight

Shawn Marshall 1/28/2021 10:29 AM

Formatted: Superscript

Naomi Ochwat 1/27/2021 9:59 PM

Deleted: 5

Naomi Ochwat 1/27/2021 9:59 PM

Deleted: 6

Naomi Ochwat 1/27/2021 9:59 PM

Deleted: 5

Luke Copland 1/25/2021 11:22 AM

Deleted: -

Shawn Marshall 1/7/2021 8:23 AM

Moved down [4]: Over the period 1979-2016, Williamson et al. (2020) reported that the St. Elias Icefield warmed at an average rate of 0.19°C decade⁻¹ at an elevation of 2000-2500 m a.s.l., rising to 0.28°C decade⁻¹ at an elevation of 5500-6000 m a.s.l.

Luke Copland 1/25/2021 11:22 AM

Deleted: -

Shawn Marshall 1/7/2021 8:23 AM

Deleted: was

Shawn Marshall 1/7/2021 8:23 AM

Deleted: a broad plateau in

Shawn Marshall 1/7/2021 8:23 AM

Moved (insertion) [4]

Shawn Marshall 1/7/2021 8:23 AM

Deleted: -

Shawn Marshall 1/7/2021 8:23 AM

Formatted: English (CAN)

Naomi Ochwat 1/27/2021 9:59 PM

Deleted: -

149 core site. Additional snow accumulation data are available from the 'Copland Camp' site on the upper Hubbard Glacier,
150 located ~12 km southwest of our drill site and at a similar elevation (Figure 1). A weather station located on a nunatak near
151 to Copland Camp has been in service since 2013 (60.70°N, 139.80°W, ~2600 m a.s.l.; Figure 1). Other relevant studies in the
152 region include ice cores collected from the Eclipse Icefield, located 12 km northwest of our drill site (Yalcin et al., 2006;
153 Zdanowicz et al., 2014) but at a higher elevation (3017 m a.s.l.).

154
155 We consider snow accumulation rates, weather conditions, and earlier firn core studies across several different locations
156 within this broad snowfield region that constitutes the upper accumulation areas of the Kaskawulsh and Hubbard Glaciers.
157 Some caution is needed in comparing different sites, but the region is relatively flat and uniform, with the exception of some
158 nunataks. Away from the nunataks there is negligible influence from topographic obstacles or valley walls, so we
159 hypothesize that the upper accumulation area will be exposed to similar climate conditions and snow accumulation rates over
160 long periods. The possibility of significant spatial variability cannot be ruled out, however, so we consider this further in the
161 data analysis.

163 3 Methods

164 3.1 Ice core field collection

165 Two 8-cm diameter cores were drilled between May 20th and 24th, 2018, using an ECLIPSE ice drill (Icefield Instruments,
166 Whitehorse, Yukon). With a starting depth of 2 m below the snow surface, Core 1 was 34.6 m long and reached a depth of
167 36.6 m, and Core 2 was 19.6 m long and reached a depth of 21.6 m. The two cores were drilled 60 cm apart, and core
168 stratigraphy and density were recorded in the field. At a depth of 34.5 m below the snow surface, liquid water became
169 evident in Core 1; drilling was stopped at a depth of 36.6 m to avoid the risk of the drill freezing in the hole.

170
171 Once the cores were retrieved the presence of ice layers, ice lenses and "melt-affected" firn was logged and the stratigraphic
172 character (e.g., texture, opacity), depth, and thickness were recorded. Melt-affected firn refers to any firn that displays
173 physical characteristics indicating that there was the presence of liquid water at some point (Figure S5). This can result in ice
174 layers, ice lenses, or can be indicated by the lack of grain boundaries, the presence of air bubbles, and opacity. When an ice
175 horizon extended across the entire diameter of the core, it was labeled as an ice layer. If the ice horizon was of more limited
176 lateral extent, it was labeled an ice lens. Ice lenses were occasionally wedge shaped.

177
178
179
180

- Shawn Marshall 1/7/2021 8:24 AM
Deleted: Many of these were undertaken
- Alison Criscitiello 1/25/2021 7:27 PM
Deleted: c
- Shawn Marshall 1/7/2021 8:24 AM
Deleted: at the Divide site
- Shawn Marshall 1/7/2021 8:25 AM
Deleted: (Figure 1)
- Shawn Marshall 1/7/2021 8:26 AM
Deleted:
- Alison Criscitiello 1/25/2021 7:27 PM
Deleted: the
- Shawn Marshall 1/7/2021 8:32 AM
Deleted: Divide site
- Alison Criscitiello 1/25/2021 7:27 PM
Deleted: c
- Shawn Marshall 1/7/2021 8:33 AM
Deleted: Divide weather station,

Naomi Ochwat 1/28/2021 7:44 PM
Moved down [1]: Each core was sawed into ~10-cm long sections in the field, and the diameter of the sections measured at each end. The sections were then double bagged, weighed, and assessed for the quality of the core sample and its cylindrical completeness, which we denote f . The average diameter was used to determine the volume of the core section (V). Together with the mass of the core section, m , density was calculated following:
$$\rho = m/V, \text{ with } V = f\pi L(D/2)^2, \text{ where } f \in [0,1] \text{ (1)}$$

where ρ is the density of the firn, D is the average core section diameter, L is the length of the section, and $f \in [0,1]$ is the subjectively assessed fraction of completeness of the core section. For example, if visual inspection indicated that about 5% of the core was missing (e.g., due to missing ice chips caused by the core dogs of the drill head), then f would be 0.95. Outliers were removed for the background firn density calculations if they were not physically possible (i.e., values $>917 \text{ kg m}^{-3}$ or $<300 \text{ kg m}^{-3}$ at depths below the last summer surface). Outliers from 32-36 m depth had residual liquid water in them, so these higher density values were retained.

215
216
217
218 All of the density measurements for Core 1 were completed in the field. The Core 2 samples could not be measured for
219 density in the field due to lack of time, so were flown to Kluane Lake Research Station frozen, where the measurements
220 were made within 24 hours of arrival. A random assortment of 125 out of the 196 Core 2 sample bags were damaged during
221 this transport, so were not included in the measurements. This left 71 samples available to use for the density analysis, with
222 at least one sample available per meter except for between 13.29 and 14.95 m. Due to these missing values, only bulk
223 density values are presented for Core 2.
224

225 3.2 Ice core density analysis

226 Ice core density measurements were completed in the field. Each core was sawed into ~10-cm long sections in the field, and
227 the diameter of the sections measured at each end. The sections were then double bagged, weighed, and assessed for the
228 quality of the core sample and its cylindrical completeness, which we denote f . The average diameter was used to determine
229 the volume of the core section (V). Together with the mass of the core section, m , density was calculated following:

$$231 \quad \rho = m/V, \text{ with } V = f\pi L(D/2)^2 \quad (1)$$

232
233 where ρ is the density of the firm, D is the average core section diameter, L is the length of the section, and $f \in [0,1]$ is the
234 subjectively assessed fraction of completeness of the core section. For example, if visual inspection indicated that about 5%
235 of the core was missing (e.g., due to missing ice chips caused by the core dogs of the drill head), then f would be 0.95.
236 Outliers were removed for the background firm density calculations if they were not physically possible (i.e., values $>917 \text{ kg}$
237 m^{-3} or $<300 \text{ kg m}^{-3}$ at depths below the last summer surface). Outliers from 32-36 m depth had residual liquid water in them,
238 so these higher density values were retained.

239
240 In order to calculate the uncertainty in density, $d\rho$, random and systematic sources of error have to be taken into account in
241 the propagation of errors:

$$242 \quad d\rho = \rho \sqrt{\left(\frac{dm}{m}\right)^2 + \left(\frac{dV}{V}\right)^2} \quad (2)$$

243 The mass uncertainty was assumed to be 0.3 g, which is a conservative estimate given the scale's accuracy ($\pm 0.1 \text{ g}$), but
244 accounts for potential residual snow or water on the scale. The volume uncertainty is calculated by breaking down Eq. (1) for
245 sample volume, $V = fAL$, where cross-sectional area $A = \pi(D/2)^2$. There is uncertainty in the measured length of the core

Naomi Ochwat 1/28/2021 7:44 PM

Moved (insertion) [1]

Naomi Ochwat 1/28/2021 7:45 PM

Deleted: Each

247 section, L , the radius of the core section, $D/2$, and the assessment of the completeness of the core sample, f . Each of these
248 was calculated independently and the propagation of uncertainty was calculated from:

249

250
$$dV = V \sqrt{\left(\frac{df}{f}\right)^2 + \left(\frac{dA}{A}\right)^2 + \left(\frac{dL}{L}\right)^2} . \quad (3)$$

251 dL was assumed to be 0.25 cm because the tape measure had ticks at every mm so it could be measured with precision, but
252 core sections were often uneven, with crumbly edges caused by the drill cutters. The same uncertainty was assigned to the
253 measurement of core diameter. Given two independent measurements, the uncertainty in the diameter is $dD =$

254 $\frac{1}{2} \sqrt{(0.25)^2 + (0.25)^2} = 0.18$ cm. For the cross-sectional area, the uncertainty $dA = \pi D dD/2$.

255

256 Values of f were determined by assessing the shape of the core and deciding how complete a cylinder the core section
257 represented (e.g., accounting for missing volume due to chips from the core dogs along the edges). Three different people
258 performed this evaluation, so there was subjectivity in each of the f values and it is best to be conservative with this estimate.
259 We assigned this to be $df = 0.2$ for $f < 0.8$ and $df = 0.1$ for $f \geq 0.8$. The uncertainty of a higher f value is lower, because when
260 a core was of good quality it was obvious. Less complete cylinders were more difficult to assess, hence the greater
261 uncertainty when $f \leq 0.8$. The f value has the greatest effect on the overall uncertainty calculation for firm density. We did not
262 record f values for Core 2 in the field, so values are based on the measurements from Core 1. The minimum value recorded
263 in Core 1 was $f = 0.7$, with a maximum of 1 and an average of 0.96. We assume a value of $f = 0.96 \pm 0.1$ for all of Core 2.

264

265 The resulting uncertainty in the density was calculated from:

266
$$d\rho = \rho \sqrt{\left(\frac{dm}{m}\right)^2 + \left(\frac{dV}{V}\right)^2} . \quad (4)$$

267 For the average densities, $\bar{\rho}$, the uncertainty can be calculated from the standard error of the mean, $d\bar{\rho} = d\rho/\sqrt{N}$, for sample
268 size N . This can be estimated from the average value of $d\rho$, but we report the more precise uncertainty calculated from the
269 root-mean square value of all point values, $d\rho_k$: $d\bar{\rho} = \frac{1}{N} [\sum_N d\rho_k^2]^{1/2}$. Density can be expressed as water equivalence (w.e.)
270 for each core section from the conversion $w = L\rho/\rho_w$, where ρ_w is the density of water. For the whole core, of length L_c , the
271 water equivalence is $w_c = L_c \bar{\rho}/\rho_w$, with units m w.e. We also include an estimate of the age of the cores, based on an
272 estimate of the average annual net accumulation rate, \bar{a} , with units m w.e. yr⁻¹. The age of the core is then $\tau_c = w_c/\bar{a}$.
273 Uncertainty is estimated by propagation of uncertainties in w_c and \bar{a} . We use an uncertainty of $dL_c = 0.5$ m for the total
274 length of the core, L_c , which is based on measurements during retrieval of Core 1 of 35.05 m from the drill panel, 34.59 m

Shawn Marshall 1/28/2021 12:54 PM

Deleted: unc

276 from the addition of core lengths, and 34.25 m from the sum of the ~10 cm samples. For Core 2 the length was 19.75 m from
277 the drill panel, 19.35 m from the addition of core lengths, and 19.63 m from the sum of the ~10 cm samples.

278
279 Ice fraction, $F_i \in [0,1]$, was calculated for each 10-cm section of the firm core. Here ice was defined based on its lack of air
280 bubbles and crystalline structure, as compared to the granular structure of firm. We refer to this as ice fraction, rather than
281 melt percent, as melt percent generally assumes that the meltwater remains within the net annual accumulation layer
282 (Koerner, 1977), which cannot be assumed here due to evidence that meltwater percolates beyond the annual accumulation
283 layer and refreezes into previous years' accumulation. The thickness of individual ice layers was summed within each 10-cm
284 core section. In core samples that had ice lenses, their diameter typically occupied about 50% of the core sample; therefore
285 their thickness was divided by two before being summed. For each core section, total ice content was divided by the length
286 of the section, L , to give F_i . These values were also summed to give the total ice core ice content.

287
288 To understand the firm densification process in the absence of refrozen meltwater, the 'background' firm density is of interest.
289 For each sample, we estimated this by subtracting the mass and volume of the ice to give the firm density in the absence of
290 ice content. We used a 30-cm moving average of total ice content and density in order to smooth out a possible error of ± 10
291 cm in assigning the location of the ice features within the stratigraphy. Each sample had a measured bulk density, ρ_b , which
292 we assume resulted from a binary mixture of ice and firm, with densities ρ_f and ρ_i . Ice and firm fractions, F_i and F_f , were
293 defined with $F_i + F_f = 1$. The background firm density was then calculated following:

294
$$\rho_f = (\rho_b - \rho_i F_i) / F_f. \quad (5)$$

295 In cases where there was no ice fraction ($F_i = 0$), $\rho_f = \rho_b$. Ice layers and lenses were assumed to have a density of 874 ± 35
296 kg m^{-3} , based on the average density of firm-core sections that were 100% ice in Greenland (873 kg m^{-3}) and Devon Ice Cap
297 (875 kg m^{-3}) (Bezeau et al., 2013; Machguth et al., 2016). This is different from the 917 kg m^{-3} upper bound used in the
298 outlier analysis because that is the theoretical limit for pure ice, whereas 874 kg m^{-3} is based on measured field data which
299 includes observed ice layers and lenses which have small bubbles and imperfections in them.

300
301 There is surface lowering associated with melting but without associated mass loss, due to subsurface refreezing. This
302 surface lowering is an 'apparent ablation' in airborne or satellite altimetry signals. We calculated this for each core section
303 using the background firm density, ρ_f , and length of the section, L . The 'thinning' or surface lowering of a given core
304 section, ΔL , was estimated by reverting the ice to the density of the background firm, following:

- Shawn Marshall 1/28/2021 1:04 PM
Deleted: Contemporary s
- Shawn Marshall 1/28/2021 1:03 PM
Deleted: refreezing
- Shawn Marshall 1/28/2021 1:12 PM
Deleted: was
- Shawn Marshall 1/28/2021 1:07 PM
Deleted: .
- Shawn Marshall 1/28/2021 1:13 PM
Deleted: For each core sample, t
- Shawn Marshall 1/28/2021 1:09 PM
Deleted: 'thinning' or
- Shawn Marshall 1/28/2021 1:11 PM
Deleted:
- Shawn Marshall 1/28/2021 1:11 PM
Deleted: associated with the total ice content, ΔL ,

$$\Delta L = L \left[\left(F_f + \frac{\rho_i F_i}{\rho_f} \right) - 1 \right]. \quad (6)$$

Summed over the full firn column, this gives the total surface lowering associated with meltwater that percolates and refreezes, with no actual loss of mass.

3.3 Historical measurements

As part of an expedition undertaken by the JRRP, Grew and Mellor (1966) measured snow density and temperature to a depth of 15 m at the Divide site on July 23, 1964 (Fig. 1). The first ~4 m were measured in a snow pit, while the remaining ~11 m were based on measurements of a core drilled with a Cold Regions Research and Engineering Laboratory (CRREL) coring auger. The original data is not available, so values were reconstructed based on digitization of the density plot provided in Figure 4 of Grew and Mellor (1966). This digitization was undertaken with WebPlot Digitizer 4.3 (Rohatgi, 2020), and has an estimated error of $\pm 2 \text{ kg m}^{-3}$ for density and $\pm 0.01 \text{ m}$ for depth. Errors were calculated by clicking the same point 25 times and evaluating the variability of the points (i.e., the standard deviation).

From July 14-17, 2006, snow density and temperature measurements were recorded every 10 cm to a depth of 10.4 m at the Copland Camp as part of a University of Ottawa field class. Measurements from 0 to 5.4 m were recorded in a snow pit, while those from 5.5 to 10.4 m were based on a core recovered with a Kovacs Mark II coring system (Kovacs Enterprises, Oregon, USA). Density measurements in the snow pit were undertaken with a 250 cm³ RIP 2 Cutter (Snowmetrics, Colorado, USA), and in the ice core by measuring and weighing core sections and using Eq. (1). Errors in the density measurements were determined from Eq. (4), and verified against density values recorded in a second snow pit dug to a depth of 4.0 m, approximately 2 m away from the first. All temperature measurements were undertaken with a Thernor PS100 digital stem thermometer with an accuracy of $\pm 0.5^\circ\text{C}$.

Annual snow accumulation at the Copland Camp was measured between 2004-2011 with a Campbell Scientific SR50 Sonic Ranging Sensor mounted on a cross-arm on a vertical steel pole drilled into the firn. The SR50 was connected to a Campbell Scientific CR10X logger, and included a correction for the change in speed of sound with air temperature. The mounting pole was raised annually to keep it above the snow surface, and densities recorded in snow pits collected during annual University of Ottawa field classes (typically in early July) were used to convert the SR50 depth measurements into w.e. values.

3.4 Energy balance and firn modelling

- Shawn Marshall 1/28/2021 1:08 PM
Deleted: This was
- Shawn Marshall 1/28/2021 1:08 PM
Deleted: s
- Shawn Marshall 1/28/2021 1:08 PM
Deleted: for
- Shawn Marshall 1/28/2021 1:08 PM
Deleted: whole core
- Shawn Marshall 1/28/2021 1:08 PM
Deleted: to give
- Shawn Marshall 1/28/2021 1:08 PM
Deleted: full amount of
- Shawn Marshall 1/28/2021 1:12 PM
Deleted: percolation
- Shawn Marshall 1/28/2021 1:12 PM
Deleted: refreezing
- Alison Criscitiello 1/25/2021 7:31 PM
Deleted: Icefield Ranges Research Project
- Alison Criscitiello 1/25/2021 7:31 PM
Deleted: CRREL (
- Alison Criscitiello 1/25/2021 7:31 PM
Deleted:)
- Naomi Ochwat 1/17/2021 7:32 PM
Deleted: and temperature
- Naomi Ochwat 1/17/2021 7:32 PM
Deleted: s
- Shawn Marshall 1/6/2021 9:15 AM
Deleted:
- Shawn Marshall 12/28/2020 5:52 PM
Deleted: .36
- Luke Copland 1/25/2021 11:31 AM
Deleted: Divide site
- Alison Criscitiello 1/25/2021 7:32 PM
Deleted: c
- Luke Copland 1/25/2021 11:32 AM
Deleted: Divide site
- Alison Criscitiello 1/25/2021 7:33 PM
Deleted: c

365 ERA climate reanalyses were used to examine changes in climate and annual surface melting at the study site since the
366 1960s, [coupled with a firn model to simulate the decadal evolution of firn temperature, hydrology, ice content, and density](#).
367 Daily melt rates were calculated from 1965 to 2019 using a surface energy balance model ([Ebrahimi and Marshall, 2016](#)),
368 coupled to a subsurface model of coupled thermal and hydrological evolution in the snow and firn ([Samimi et al., 2020](#)). The
369 model calculates the surface energy budget and snow melt based on incoming shortwave and longwave radiation,
370 temperature, relative humidity, wind speed, and air pressure, with internal parameterizations of surface albedo evolution and
371 outgoing longwave radiation. Conductive heat flux to the snow surface and snow surface temperatures [are simulated within](#)
372 the subsurface snow/firn model. [Snow and firn densification are parameterized following Vionnet et al. \(2012\) for the firn](#)
373 [matrix \('background firn'\), with bulk density including the additional mass of any ice or water content. Details of the model](#)
374 [are provided in the Supplementary Information](#).

Shawn Marshall 1/6/2021 9:16 AM
Deleted: Ebrahimi and Marshall, 2016;

Shawn Marshall 1/6/2021 9:17 AM
Deleted: were

375
376 Meteorological inputs for the surface energy balance model were derived from the ERA5 climate reanalysis for the period
377 1979 to 2019 (Hersbach et al., 2020), and extended back to 1965 using the ERA 20th century reanalysis (ERA20c; Poli et al.,
378 2016). ERA5 outputs are at a resolution of 0.25° latitude and longitude, and data for our analysis was averaged from ERA5
379 grid cells located at (60.75°N, 139.75°W) and (60.75°N, 139.5°W). ERA20c data are at 1° latitude and longitude resolution,
380 and we interpolated meteorological conditions to [the upper Kaskawulsh Glacier](#) from the four model grid cells at 60° to
381 61°N and 139° to 140°W. ERA20c fields were homogenized with ERA5 through bias adjustments for two years of overlap
382 in the reanalyses, 1979 and 1980, with ERA5 assumed to be the more accurate reconstruction. Monthly bias adjustments
383 based on this period of overlap were then applied to the ERA20c data from 1965 to 1978.

Shawn Marshall 1/7/2021 9:53 AM
Deleted: our study site

384
385 [The reanalysis data represent the climatology over the region of the upper Kaskawulsh-Hubbard divide \(i.e., a 0.25° grid](#)
386 [cell\), and are not specific to our core site. The firn modelling is therefore taken to be generally applicable for this upper](#)
387 [plateau region. However, ERA meteorological conditions \(temperature, pressure, humidity\) are bias-adjusted to the specific](#)
388 [elevation of our core site, 2640 m.](#) ERA5 temperature fields were evaluated against [Copland](#) weather station data from 2014-
389 2018, which indicate a small (0.6°C) cold bias in the ERA5 data for average summer (JJA) temperatures over this period.
390 ERA temperatures were [further](#) bias-adjusted by this amount. [Our core site, the Copland weather station, Copland Camp, and](#)
391 [IRRP research sites all fall within the same ERA5 grid cell, and we make the assumption that climate conditions are similar](#)
392 [for similar elevations and glaciological settings within this region.](#)

Shawn Marshall 1/7/2021 9:57 AM
Deleted: -

Luke Copland 1/25/2021 11:47 AM
Deleted: Divide

Shawn Marshall 12/28/2020 6:15 PM
Deleted: d

Luke Copland 1/25/2021 11:48 AM
Deleted: and

Alison Criscitiello 1/25/2021 8:00 PM
Deleted: c

393
394 Surface energy balance and melt were calculated every 30 minutes, using mean daily meteorological forcing [from ERA](#) and
395 a parameterization of the diurnal cycles of temperature [and](#) incoming shortwave radiation ([Ebrahimi and Marshall, 2016](#)).

Shawn Marshall 1/6/2021 9:19 AM
Deleted: , humidity,

396 [Subsurface temperatures were modelled for a 35-m firn column](#), with a simple model for meltwater percolation that accounts
397 for meltwater refreezing and the associated latent heat release where snow or firn is below 0°C ([Samimi and Marshall, 2017](#);

Shawn Marshall 1/7/2021 10:12 AM
Deleted: -

Shawn Marshall 12/28/2020 6:13 PM
Deleted: the upper 20 m of the

410 Samimi et al., 2020). For the current study, we discretize the snow and firn into 58 layers, from 0.1 to 1 m in thickness, with
411 higher resolution near the surface. The firn model is coupled with the surface energy balance model, solving for the firn
412 thermodynamic and hydrological evolution at 30-minute time steps for the period 1965 to 2019. The subsurface temperature
413 evolution includes vertical heat conduction and latent heat release from refreezing. When subsurface temperatures reach 0°C,
414 liquid water is retained or percolates to depth, following a Darcian parameterization for water flux: $q_w = -k_w \nabla \phi$, for hydraulic
415 conductivity k_h and hydraulic potential ϕ (Samimi and Marshall, 2017). For the numerical experiments in this study we set k_h
416 = 10^5 m s^{-1} in snow and 10^6 m s^{-1} for snow and firn, respectively. Capillary water retention is calculated following Coléou
417 and Lesaffre (1998). The default model parameters are based on calibration at DYE-2, Greenland, in the percolation zone of
418 the southern Greenland Ice Sheet (Samimi et al., 2020). A broader range of model parameters is explored in sensitivity
419 analyses presented in the Supplementary Information.

420
421 The model is 'spun up' through a 30-year simulation with perpetual 1965 climate forcing (i.e., running through 30 annual
422 cycles with 1965 climate conditions). This provides the initial temperature, density, and ice-layer structure within the firn
423 column. Sensitivity tests within the Supplementary Information also examine the model sensitivity to these initial conditions
424 and the spin-up assumptions.

426 4 Results

427 4.1 Ice core density

428 The density data are plotted in Figure 2, fitted with a logarithmic curve to quantitatively compare our two cores. The first 4.2
429 m of both 2018 cores was dry and had an average density of $450 \pm 21 \text{ kg m}^{-3}$, with no ice content. At 4.2 m there was a
430 significant ice crust, with large crystal size, rounded grains and high impurity content, which was assumed to represent the
431 last summer surface (LSS) from 2017. The snow above this LSS layer was therefore classified as seasonal snow. In this
432 section we focus on the firn characteristics below the LSS, so our discussion is centered on the core recovered between 4.2
433 and 36.6 m below the surface for Core 1 (i.e., total firn length of 32.4 m), and between 4.2 and 21.6 m below the surface for
434 Core 2 (i.e., total firn length of 17.4 m). For consistency, we reference all depths to the seasonal snow surface throughout
435 this paper.

436
437 In the upper 10 m of firn (4.2 to 14.2 m below the surface; Table 1), Cores 1 and 2 had average densities of $588 \pm 8 \text{ kg m}^{-3}$
438 and $572 \pm 7 \text{ kg m}^{-3}$, respectively, giving an overall average density of $580 \pm 5 \text{ kg m}^{-3}$. Over the upper 17.4 m of firn in each
439 core (4.2 m to 21.6 m below the surface; the depth to the bottom of Core 2), Kaskawulsh firn had an average density of 632
440 $\pm 4 \text{ kg m}^{-3}$. The full 32.4 m of firn at Core 1 (4.2 to 36.6 m below the surface) had an average density of $698 \pm 5 \text{ kg m}^{-3}$. Ice
441 content generally increased with depth in the upper ~25 m of the core, but deeper sections were less icy (Table 1). The

Shawn Marshall 12/28/2020 6:17 PM

Deleted: The model

Shawn Marshall 12/28/2020 6:17 PM

Deleted: s

Shawn Marshall 12/28/2020 6:13 PM

Deleted: 43

Shawn Marshall 1/19/2021 9:23 AM

Deleted: ,

Shawn Marshall 12/28/2020 6:17 PM

Deleted: It was

Shawn Marshall 1/28/2021 8:03 PM

Deleted: , heat advection from meltwater percolation,

Shawn Marshall 1/6/2021 9:20 AM

Deleted: w

Shawn Marshall 1/6/2021 9:21 AM

Deleted: We

Shawn Marshall 1/6/2021 9:22 AM

Deleted: , for the numerical experiments in this study

Shawn Marshall 12/28/2020 6:14 PM

Deleted: was

Shawn Marshall 1/6/2021 9:20 AM

Deleted: e

Luke Copland 1/25/2021 11:49 AM

Deleted: s

Luke Copland 1/25/2021 11:49 AM

Deleted: i

Luke Copland 1/25/2021 11:50 AM

Deleted: s

Luke Copland 1/25/2021 11:50 AM

Deleted: i

Shawn Marshall 1/6/2021 10:20 AM

Formatted: English (UK)

Shawn Marshall 1/6/2021 9:25 AM

Deleted:

Shawn Marshall 1/6/2021 9:25 AM

Moved (insertion) [2]

Shawn Marshall 1/6/2021 9:26 AM

Deleted: To make comparisons with Sorge's Law of densification (Bader, 1954), a logarithmic curve was fitted to the density data in Figure 2.

Shawn Marshall 1/6/2021 9:25 AM

Moved up [2]: To make comparisons with Sorge's Law of densification (Bader, 1954), a logarithmic curve was fitted to the density data in Figure 2.

467 bottom 5 m of firm in Core 1 had an average density of $826 \pm 13 \text{ kg m}^{-3}$, but with no identified ice layers. Based on the high
468 density and texture of this deep firm, along with the presence of liquid water in the deepest sections of the core, we believe
469 that we drilled to near the base of the firm at the core site, but cannot confirm this as we halted drilling before reaching
470 glacier ice.

471
472 Total ice content in the 32.2 m firm portion of Core 1 (4.2 to 36.6 m below the surface) was $2.33 \pm 0.26 \text{ m}$ of ice or $2.67 \pm$
473 0.24 m w.e. This is equivalent to 7.2% by volume and 11.9% by mass (Table 1). Using Eq. (5) and the values for ice content
474 in Core 1, we estimate a background firm density of $676 \pm 6 \text{ kg m}^{-3}$ for the full column of firm, 3.2% less than the bulk density
475 of the firm (Table 1). The two cores had very similar bulk and background densities over the upper 10 m of firm (4.2 to 14.2
476 m below the surface) and 17.4 m (4.2 to 21.6 m below the surface), where a direct comparison was possible. The total water
477 equivalent of firm in Core 1 was calculated to be $w_e = 22.5 \pm 0.2 \text{ m w.e.}$
478

479 4.2 Ice core stratigraphy

480 The stratigraphy of the 2018 cores indicates numerous ice layers ~~as well as melt-affected firm, distinguished by a lack of~~
481 ~~grain boundaries or opaque, bubbly firm.~~ The first 4.2 m comprised the seasonal snowpack, with firm below. Within the first 6
482 m below the surface there were several small ice layers (<2.5 cm thick), interpreted as wind crusts (Figure 3). Several thick
483 (>10 cm) ice layers were found between 6 and 26 m depth (1.8 to 21.8 m in the firm). The largest ice layer in Core 1 was 22
484 cm thick, found at 14.1 m (9.9 m in the firm). At 26.4 m (22.2 m in the firm) the ice layers and lenses disappeared. Below this
485 the firm was almost entirely meltwater-affected, based on its appearance and texture, but without the quantity of ice lenses or
486 ice layers that were present in the first 25 m. We interpret this section of the core as infiltration ice, consisting of water-
487 saturated firm that has experienced refreezing. At 30 m depth (25.8 m in the firm), the meltwater effects were absent and there
488 were two small ice layers and an ice lens. At 30.6 m depth the firm was melt-affected again. From 34.5 to 36.6 m (30.3 to
489 32.4 m in firm) the core sections expelled liquid water as they were extracted from the core barrel.

490
491 In Core 2 there were numerous ice layers starting at a depth of 3.8 m, and below 4.4 m (0.2 m in the firm) the core was
492 meltwater-affected. There was a thick ice layer at 6.6 m (2.4 m in the firm) that was 30 cm lower than a similar ice layer in
493 Core 1 at 6.3 m. There were numerous melt-affected layers between ice lenses much closer to the surface in Core 2 than
494 Core 1. In Core 1 there were several ice layers at ~10 m depth (5.8 m in the firm), but these layers were not present in Core 2.
495 At 14.4 m (10.2 m in the firm) another section of the firm had numerous ice layers (~20-30 cm deeper than recorded in Core
496 1), and at 14.6 m the thickest ice layer was encountered (12 cm), corresponding well with the thickest layer in Core 1.
497 Between 16 and 21.5 m (11.8 to 17.3 m in the firm) the core was melt-affected. We attribute differences between Core 1 and
498 Core 2 stratigraphy to uncertainty in the depth of features (as discussed in Section 3.2), and horizontal variability in
499 meltwater infiltration, which is known to occur at length scales less than 1 m (Parry et al., 2007; Harper et al., 2011).

Shawn Marshall 1/28/2021 8:12 PM

Deleted: and

Shawn Marshall 1/28/2021 8:14 PM

Deleted: . Melt-affected firm is

Shawn Marshall 1/28/2021 8:13 PM

Deleted: ice layers, ice lenses, or can be indicated by the

Shawn Marshall 1/28/2021 8:13 PM

Deleted: , the presence of air bubbles, and opacity

505

506 **4.3 Changes in firn characteristics over time**

507 The firn in the accumulation area of Kaskawulsh Glacier has become denser since 1964 (Figure 4a). The mean density of the
508 upper 7 m of firn was 516 kg m⁻³ in 1964 (3.3 to 10.3 m below the surface), 590 kg m⁻³ in 2006 (3.5 to 10.5 m below the
509 surface) and 549 kg m⁻³ in 2018 (4.4 to 11.4 m below the surface). The difference between the average densities from the
510 upper 7 m in the 1964 and 2018 core is 33 kg m⁻³, which is an increase of ~7%. It is difficult to assess whether firn
511 temperatures have changed over this time, as limited data are available from below the depth of the annual temperature wave
512 (~10 m for heat diffusion, and deeper than this with the effects of subsurface meltwater infiltration and latent heat release).
513 Borehole temperature records from Grew and Mellor (1966) indicate temperate (0°C) conditions at 15-m depth in the
514 summer of 1964, which suggests that deep temperate firn may have existed at this site in the 1960s. This supports the
515 assumption that Kaskawulsh Glacier is temperate (Foy et al., 2011), despite mean annual air temperatures of about -11°C on
516 the upper glacier.

517

518 Accumulation data from the IRRP A site, Copland Camp, and our 2018 measurements do not show any evidence for a
519 significant change over time, although there can be high interannual variability. At IRRP A, Wagner (1969) reported values
520 between 1.3 m to 1.9 m w.e. yr⁻¹ for 1963. Marcus and Ragle (1970) measured a winter snow accumulation of 1.6 m w.e.
521 from 1964-1965. Holdsworth (1965) reported an estimated mean annual accumulation rate of 1.8 m w.e. yr⁻¹ in the early
522 1960s (year not specified) (Holdsworth, 1965). Yearly snow accumulation data from 2004-2011 collected with the SR50 at
523 Copland Camp indicate a mean annual accumulation rate of 1.77 m w.e. yr⁻¹, with variations between 1.3 and 2.4 m w.e. yr⁻¹.
524 The seasonal snowpack at our drill site was 4.2 m in May 2018, with an average snow density of 440 kg m⁻³, giving a total
525 accumulation of 1.85 m w.e. for 2017-18.

526

527 Based on the above review, we adopt an estimate of $\bar{a} = 1.8 \pm 0.2$ m w.e. yr⁻¹ for the net accumulation from 2005 to 2018.
528 Using this value, the firn layer of Core 1 represents 12.5 ± 1.4 years of net accumulation (i.e., 2005-2017), or 13.2 ± 1.4 years,
529 if the seasonal snowpack on top is counted. Over 12.5 years, the total measured ice content of 2.67 m w.e. in the firn equates
530 to an average meltwater refreezing rate of 0.22 m w.e. yr⁻¹.

531

532 **4.4 Surface energy balance and firn modelling**

533 Reconstructed air temperature, melt, and firn trends from 1965-2019 are shown in Figure 5. Summer air temperature from
534 the reanalysis (Figure 5A) shows a modest but statistically significant increase over the study period, with a trend of +0.07°C
535 decade⁻¹. Table 2 reports changes in meteorological, energy balance, and modelled firn conditions over this time. Specific
536 humidity and incoming longwave radiation increase markedly over the 55 years, with trends of +0.1 g kg⁻¹ decade⁻¹ and +3.5

- Shawn Marshall 1/3/2021 7:25 PM
Deleted: To start with, the seasonal snowpack over a depth of 3.28 m in 1964 had a mean density 472 kg m⁻³, compared to a density 655 kg m⁻³ over the seasonal snowpack depth of 3.50 m in 2006. Below this, ... t...e mean firn ...ensity over the depthl ... [7]
- Naomi Ochwat 1/28/2021 8:03 PM
Deleted: 92...kg m⁻³ in 2018 (4.42 ... [8]
- Naomi Ochwat 1/28/2021 8:03 PM
Deleted: 2
- Shawn Marshall 1/28/2021 8:20 PM
Moved down [5]: The difference between the average densities from 5-15 m in the 1964 and 2018 core is 8.5 kg m⁻³.
- Shawn Marshall 1/28/2021 8:20 PM
Moved (insertion) [5]
- Shawn Marshall 1/3/2021 7:26 PM
Deleted: -
- Shawn Marshall 1/3/2021 7:27 PM
Deleted: When the seasonal snowpack is excluded to enable comparison between all three measurement periods, t
- Naomi Ochwat 1/28/2021 9:58 PM
Deleted: There is a cumulative difference in water equivalent content of the firn pack of 0.53 m w.e. over the depth range of the first 7 m of firn, indicating (3 to 10 m or 4 to 11 m below the ... [9]
- Naomi Ochwat 1/28/2021 8:04 PM
Deleted: 5-15...pper 7 m in the 1964 and ... [10]
- Shawn Marshall 1/3/2021 7:33 PM
Deleted: - ... [11]
- Shawn Marshall 1/3/2021 7:50 PM
Deleted: The a
- Luke Copland 1/25/2021 2:48 PM
Deleted: Divide
- Alison Criscitiello 1/25/2021 8:05 PM
Deleted: c
- Luke Copland 1/25/2021 2:48 PM
Deleted: site
- Shawn Marshall 1/3/2021 7:49 PM
Deleted: is sometimes...an be high interar ... [12]
- Luke Copland 1/25/2021 2:49 PM
Deleted: at the Divide site ...n the early 19... [13]
- Alison Criscitiello 1/25/2021 8:07 PM
Deleted: c
- Shawn Marshall 1/3/2021 7:51 PM
Deleted: d...a mean annual accumulation ... [14]
- Shawn Marshall 1/16/2021 10:39 AM
Deleted: and ...melt, and firn trends from ... [15]

641 W m² decade⁻¹, respectively. This echoes the findings of Williamson et al. (2020), who report decadal-scale, high-elevation
 642 warming in the St. Elias Mountains in association with increases in atmospheric water vapour and longwave radiation. These
 643 trends augment the net energy available for melt, through increases in both the net radiation and latent heat flux. Modelled
 644 annual melt averaged 230±210 mm w.e. yr⁻¹ from 1965 to 2019 and 380±310 mm w.e. yr⁻¹ from 2005 to 2017, 70% higher
 645 than the long-term average. The latter interval represents the approximate period of record of the firn core. The trend in
 646 surface melting is +62 mm w.e. yr⁻¹ decade⁻¹ from 1965 to 2019 (Figure 5B). The summer of 2013 was exceptional; it had
 647 the warmest summer temperatures on record, T_{MA} = -0.7°C, with 895 mm w.e. of meltwater (Table 2).
 648
 649 Within the model, 91% of the surface meltwater refreezes in the firn over the period 1965-2019, with 100% of it refreezing
 650 in cool summers when meltwater generation is limited. Meltwater that does not refreeze percolates to depth in the firn
 651 model. Figure 5B plots the annual melting minus refreezing, with positive values indicating deep percolation. If the firn is
 652 temperate (0°C), meltwater can percolate through the entire depth of the firn column (35 m), where it is permitted to “drain”
 653 through the lowest layer; this water leaves the system and is considered as runoff. Porewater in the firn also refreezes in the
 654 subsequent winter, to the depth of the winter cold wave, accounting for the negative values in Figure 5B. This represents
 655 percolated meltwater that refreezes within the firn column in the following calendar year. Complete meltwater retention is
 656 typical for most of the period from 1965 to the early 2010s, but there is a marked increase in modelled runoff over the last
 657 decade (Figure 5B), indicating drainage through the full 35-m firn column. Only 73% of surface melt refroze during the
 658 period 2005-2017, and the mass loss associated with summer mass balance increased five-fold, from an average of -20±120
 659 mm w.e. yr⁻¹ from 1965-2019, to -105±220 mm w.e. yr⁻¹ from 2005-2017.
 660
 661 Summers with high amounts of surface melt produce greater refreezing and warming of the snow and firn, eventually
 662 overwhelming the cold content and enabling deep percolation and drainage. Figures 5C and 5D plot the modelled evolution
 663 of the firn temperatures and the wetting and melting fronts, which closely coincide. Snow and firn temperatures in Figure 5C
 664 are mean annual values at the snow surface (the upper 0.1 m), and at 10, 20, and 35 m depth. For a purely conductive
 665 environment, ~10 m represents the depth of the annual temperature wave (Cuffey and Paterson, 2010), but latent heat release
 666 from meltwater refreezing warms the subsurface and causes a deeper influence of surface conditions, such that 10-m
 667 temperatures are highly variable (Table 2). The modelled wetting and melting fronts in Figure 5D suggest dramatic recent
 668 developments in firn thermal and hydrological structure at the Kaskawulsh drill site, with a regime shift in the firn structure
 669 over the period 2013-2017. This is consistent with the birth of a deep PFA at this time. Figure 6 plots the full subsurface
 670 temperature evolution over the period 1965-2019, showing the typical seasonal evolution of firn temperatures and the
 671 unusual nature of the hydrological breakthrough event that began in 2013 and persists through 2019. Figures 5E and 5F plot
 672 the modelled increases in average firn density and total firn ice content from 1965-2019. The average firn density in the
 673 model is 682 kg m⁻³ in 2018, compared to 698±5 kg m⁻³ measured in Core 1.

- Shawn Marshall 12/28/2020 6:27 PM
Deleted: who attributed ...decadal-scale, ... [16]
- Shawn Marshall 1/6/2021 9:37 AM
Deleted: 154 ...10 mm w.e. yr⁻¹ from 1965 ... [18]
- Luke Copland 1/25/2021 2:50 PM
Deleted: was
- Shawn Marshall 1/16/2021 10:43 AM
Deleted: 231 ±242 mm w.e. yr⁻¹ from 2005 to 2017 ...80 ± 310 mm w.e. yr⁻¹ ... from 2005 ... [19]
- Shawn Marshall 1/6/2021 9:37 AM
Formatted: ... [17]
- Luke Copland 1/25/2021 2:50 PM
Deleted: waswith
- Shawn Marshall 1/6/2021 9:42 AM
Deleted: and ...ith 766 ... [20]
- Shawn Marshall 1/6/2021 9:34 AM
Deleted: Our m...ithin the model results i... [21]
- Naomi Ochwat 12/19/2020 6:48 AM
Deleted: which
- Shawn Marshall 1/6/2021 9:46 AM
Deleted: can drain laterally, but most of it... [22]
- Luke Copland 1/25/2021 2:51 PM
Deleted:
- Shawn Marshall 1/6/2021 9:47 AM
Deleted: 6b...), indicating drainage throug... [23]
- Shawn Marshall 1/6/2021 9:58 AM
Formatted: ... [24]
- Shawn Marshall 1/6/2021 9:58 AM
Deleted: 42 ...20 mm w.e. yr⁻¹ from 1965... [25]
- Shawn Marshall 1/6/2021 9:58 AM
Deleted: 98
- Shawn Marshall 1/6/2021 9:58 AM
Formatted: ... [26]
- Shawn Marshall 1/19/2021 9:25 AM
Deleted: resulted in ...roduce greater refre... [27]
- Naomi Ochwat 1/28/2021 10:21 PM
Deleted: firn aquifer
- Shawn Marshall 1/6/2021 10:01 AM
Deleted: 7 ... plots the full subsurface tem... [28]

766 The model results in Figures 5 and 6 are for the 'reference' 1965-2019 ERA climatological forcing and firm model
 767 parameters. These are the direct ERA climate fields, bias-adjusted to represent the elevation of the core site and to give
 768 consistency with the regional Copland weather station data (2014-2018). The weather station has a similar elevation and
 769 topoclimatic environment and is about 11 km from the core site, falling within the same ERA5 grid cell. Firm model settings
 770 are based on calibrations against field data at DYE-2, Greenland, within the percolation zone of the southern Greenland Ice
 771 Sheet (Samimi et al., 2020), but we have no local field calibration of these model parameters. There are therefore
 772 uncertainties within both the climate forcing and the model parameters and assumptions. The Supplemental Information
 773 examines the sensitivity of model results to several important meteorological inputs and model parameters, as well as the
 774 strategy adopted for the model spin-up.
 775
 776 Select results are plotted in Figure 7, indicating the wide range of model behaviour that is possible with perturbations to the
 777 model inputs, parameter settings, and spin-up assumptions. An air temperature anomaly of $\pm 1^\circ\text{C}$ applied to the reference
 778 ERA climatology gives very different firm evolutions from 1965-2019, with warmer temperatures driving a shift to temperate
 779 firm conditions in the late 1980s (Figures 7A and C). Warming of 2°C gives temperate firm for the entire period. In the other
 780 direction, a temperature anomaly of -1°C is sufficient to maintain perpetual polythermal conditions at the site, precluding
 781 the development of deep temperate firm or a PFA. Similar results are attained with perturbations of $\pm 10 \text{ W m}^{-2}$ to the
 782 incoming longwave radiation (Supplemental Information). Increases in meltwater infiltration that are stimulated by lower
 783 values of the irreducible water content ($\theta_{wi} < 0.025$) have a similar effect to warming, promoting meltwater infiltration, firm
 784 warming, and the earlier development of temperate firm.
 785
 786 The simulations are also sensitive to the initial conditions (Figures 7B and D). Given evidence from Grew and Mellor (1966)
 787 that firm at 15-m depth was temperate in the mid-1960s near our core site, we introduce temperature anomalies from $+0.5$ to
 788 $+2^\circ\text{C}$ to the spin-up climatology. A perturbation of $+1.5^\circ\text{C}$ creates temperate conditions to 12-m depth, and $+2^\circ\text{C}$ is
 789 sufficient to create deep temperate firm which persists for several years (Figure 7D). Firm refreezes in the 1970s within the
 790 model, and eventually follows a similar path to the reference simulation, but with a memory of warmer initial firm
 791 temperatures. This permits a more rapid transition (or return) to deep temperate conditions spurred by the heavy melt season
 792 in 2013. Overall, the model sensitivities in Figure 7 indicate that a wide range of model solutions is possible at this site,
 793 indicating that Kaskawulsh Glacier firm is very close to the threshold for either temperate or polythermal conditions. We
 794 discuss this further below.
 795
 796 The initial firm density and ice content are relatively high when we force the model to produce temperate firm conditions in
 797 the mid-1960s through an air temperature anomaly of $+2^\circ\text{C}$ in the model spin-up. Values in 1965 are 679 kg m^{-3} and 2.8 m .

Alison Criscitiello 1/25/2021 8:22 PM
 Deleted: AWS
 Alison Criscitiello 1/25/2021 8:22 PM
 Deleted: AWS

Luke Copland 1/25/2021 2:54 PM
 Deleted: ry
 Luke Copland 1/25/2021 2:54 PM
 Deleted: Material

Naomi Ochwat 1/28/2021 10:21 PM
 Deleted: firm aquifer
 Shawn Marshall 1/6/2021 10:43 AM
 Formatted: Font:6 pt
 Shawn Marshall 1/6/2021 10:42 AM
 Formatted: Font:6 pt
 Shawn Marshall 1/6/2021 10:42 AM
 Formatted: Superscript
 Shawn Marshall 1/6/2021 10:42 AM
 Formatted: Superscript
 Luke Copland 1/25/2021 2:54 PM
 Deleted: s
 Luke Copland 1/25/2021 2:54 PM
 Deleted: ry
 Luke Copland 1/25/2021 2:54 PM
 Deleted: material
 Shawn Marshall 1/6/2021 10:44 AM
 Formatted: Font:Italic, Subscript
 Shawn Marshall 1/6/2021 10:13 AM
 Deleted:
 Shawn Marshall 1/19/2021 10:06 AM
 Formatted: Font:6 pt
 Shawn Marshall 1/19/2021 10:05 AM
 Formatted: Superscript
 Shawn Marshall 1/19/2021 10:05 AM
 Formatted: Superscript

808 compared with reference model values of 641 kg m^{-3} and 0.7 m. Figure 8 plots the subsequent firn temperature and density
809 evolution if the $+2^\circ\text{C}$ temperature anomaly is maintained from 1965 to 2019 and in the case where the model forcing is
810 restored to the reference ERA climatology from 1965 to 2019. Subsurface temperature and density evolutions in the latter
811 case parallel that of the reference model after a transient adjustment period of about a decade, while the perpetual $+2^\circ\text{C}$
812 anomaly maintains dense and temperate firn. The decadal adjustment of firn density (Figure 8B) is the 'over-turning' time of
813 the firn core, for downward advection of new snow and firn to 35 m depth. The temperature adjustment (Figures 8A,C) does
814 not follow this as it is governed by thermal diffusion time scales in the deep firn, giving a longer memory of the initial
815 conditions.

816

817 5 Discussion

818 5.1 Firn characteristics and changes over time

819 The accumulation area of Kaskawulsh Glacier currently has indications of widespread meltwater percolation and refreezing.
820 Meltwater is stored within the firn as ice, as indicated by the presence of ice layers and infiltration ice, and there is liquid
821 water at a depth of ~ 35 m below the surface. The density of the firn has increased by about 1.5% since 1964 in the first 7 m
822 of firn, due to the increased presence of ice layers. However, the firn in 1964 was not without meltwater percolation and
823 refreezing; Grew and Mellor (1966) note the presence of refrozen ice lenses and glands and report evidence for meltwater
824 infiltration and refreezing at depths of ~ 5 m. Nevertheless, the quantity and thickness of ice layers and lenses have increased
825 towards present day, as reflected in the changes in the stratigraphy and the density (Figure 4). The firn modelling also
826 indicates decadal-scale increases in firn ice content and density (Table 2, Figure 5E). For the reference model parameter
827 settings and ERA climate forcing, the model predicts a significant increase in melting (Figure 5B), driving increases in the
828 depth of the melting and wetting fronts, meltwater percolation and runoff, and latent heat release associated with refreezing
829 since the 1960s. This fundamentally changes the way the firn contributes to the mass balance of the glacier and englacial
830 hydrological dynamics, as discussed further in section 5.3. There are significant decadal firn warming trends in the model
831 (Figures 5 and 6), driven by the increases in melting and meltwater percolation. The modelling is not observationally
832 constrained, however (Figure 7 and Supplementary Material), so the simulated firn warming is uncertain.

833

834 Increased firn meltwater and ice content, as well as potential firn warming in recent decades, will affect firn densification
835 processes. Melting rounds snow grains and increases the rate of the first stage of densification. With enough melt to drive
836 meltwater percolation through the snow and firn layer, meltwater can fill in air pockets and refreeze, further accelerating the
837 transition from snow to ice (Cuffey and Paterson, 2010). The overall pattern of density measurements from 2018 resembles a
838 logarithmic densification curve (Figure 2) (Cuffey and Paterson, 2010), as is typical for Sorge's Law of densification in dry

Shawn Marshall 1/28/2021 10:35 AM

Deleted: 1965-2019

Alison Criscitiello 1/25/2021 8:11 PM

Deleted: s

Naomi Ochwat 12/19/2020 6:50 AM

Deleted: These characteristics of the firn have changed since 1964.

Shawn Marshall 1/7/2021 8:57 AM

Deleted: 14...5% since 1964 in the first 7 ... [29]

Naomi Ochwat 12/19/2020 6:51 AM

Deleted: and temperature

Shawn Marshall 1/6/2021 11:17 AM

Deleted: The snow and firn temperature has also increased since 1964, by an average of 1.7°C . This has resulted in the removal of the winter cold wave by July 2006, with similar temperatures measured in seasonal snowpits dug in July since then at the Divide site... The melt modeling confirms th... [30]

Shawn Marshall 1/6/2021 1:26 PM

Deleted: The warming and densification of the firn has the potential to affect densification processes, and as the presence of... increased firn meltw... [31]

Luke Copland 1/25/2021 3:12 PM

Deleted: typical

Shawn Marshall 1/6/2021 1:31 PM

Deleted: expected given

910 snow (Sorge, 1935; Bader, 1954). However, with increasing meltwater percolation and refreezing effects, higher densities
911 are common in the upper portions of the firn, as observed in our cores. Bezeau et al. (2013) report similar findings from the
912 Devon Ice Cap, where they found a depth-density reversal and suggest that Sorge's Law no longer holds in areas of
913 significant warming. To account for this, firn densification models are being revised to address the effects of ice layers and
914 warming temperatures on the rate of densification (Reeh, 2008; Ligtenberg et al., 2011), and other studies are revising mass
915 balance estimates based on dynamic densification rates (e.g., Schaffer et al., 2020).

916

917 5.2 Perennial Firn Aquifer

918 We found unequivocal evidence for a deep perennial firn aquifer on the Upper Kaskawulsh Glacier, with excess water in the
919 firn pore space below about 32 m depth. Some of this water drained during firn core acquisition (Supplemental material
920 video 1 & 2). We cannot tell whether this PFA is a new feature at this site. Borehole temperature measurements from 1964 at
921 a site close to our cores indicate temperate conditions at 15-m depth at this time (Grew and Mellor, 1966), and it is possible
922 that firn has been temperate since that time, conducive to a PFA below the depth of the annual winter cold wave. There are
923 no historical temperature measurements from greater firn depths at the site, and earlier coring efforts and radar surveys from
924 the upper Kaskawulsh, Divide, or Eclipse sites make no comment or inference about the presence of liquid water, so we
925 cannot attest to the age or origins of the PFA. It may well be a new feature.

926

927 The modelling results suggest that there are significant decadal increases in melting and refreezing since the 1960s at this
928 site, driving firn warming, increased ice content, and densification (Table 2). The firn model predicts the development of
929 wet, temperate conditions in the deep firn following the 2013 melt season, although it takes four years to fully develop
930 (Figure 6). This was triggered by meltwater penetration to 11 m depth in 2013, which is below the depth of penetration of the
931 winter cold wave. Temperate conditions propagated downwards in the following years and persisted to 2019, supported by
932 several more years with above-average melting. Deep meltwater percolation during these years would support the
933 development and recharge of a PFA or perched water table at the glacier ice-firn interface. This agrees with the stratigraphy
934 found in the field. The presence of firn that has not been visibly affected by meltwater overlying the PFA implies that deep
935 meltwater infiltration through vertical piping may be an important process here and may allow the PFA to be recharged in a
936 heavy melt season. In the model, deep recharge does not occur every summer after the establishment of a temperate firn
937 column; the summer melt still needs to break through the winter cold layer, which typically extends to 6-7 m depth (Figure
938 6). Also of interest in Figure 6 is a large melt event in 2007, which led to meltwater infiltration and warming to about 9-m
939 depth. This was similar to the 2013 melt event, but the summers of 2008 to 2010 were relatively cool (average JJA
940 temperatures of -2.8°C and melting of 111 mm w.e.), leading to refreezing in the upper 9 m of firn. Thawing of the full 35-
941 m firn column to shift it from polythermal to temperate conditions requires several years of sustained melt forcing in the
942 model.

943

Shawn Marshall 1/6/2021 1:31 PM

Deleted: , even though there is large scatter in the density values, and a large uncertainty associated with each point... [32]

Naomi Ochwat 12/19/2020 6:56 AM

Deleted: as ...eltwater percolation and refi... [33]

Shawn Marshall 1/6/2021 1:31 PM

Deleted:

Naomi Ochwat 12/19/2020 6:56 AM

Deleted: continue

Shawn Marshall 1/6/2021 1:31 PM

Deleted: this density curve is likely to reverse, with... higher densities are common in the u... [34]

Naomi Ochwat 1/17/2021 8:44 PM

Deleted: a

Naomi Ochwat 1/28/2021 10:21 PM

Deleted: firn aquifer...FA is a new feature... [35]

Shawn Marshall 1/6/2021 2:02 PM

Deleted: Increased...melting and refreez... [36]

Shawn Marshall 1/6/2021 2:06 PM

Moved (insertion) [3]

Shawn Marshall 1/6/2021 2:06 PM

Deleted: ed...the development of wet, ten... [37]

Naomi Ochwat 1/28/2021 10:21 PM

Deleted: firn aquifer

Shawn Marshall 1/28/2021 11:30 AM

Deleted: , assuming that glacier ice represents an impermeable barrier at the base of the firn... [38]

1012 There are significant uncertainties in the modelling, associated with the climatological forcing, surface energy balance and
 1013 firm model parameterizations, and initial conditions. The Supplemental Information explores these in detail, while Figure 7
 1014 provides an illustration of the range of simulated behaviour for different model settings. The ‘reference model’ results
 1015 presented in Figures 5 and 6 should be seen as just one scenario, corresponding to our best estimate of the parameter settings.
 1016 We lack local calibration and validation studies, so we cannot preclude different firm temperature and melt evolutions at this
 1017 site, particularly given the inference of Grew and Mellor (1966) that firm at 15-m depth was temperate in the mid-1960s. The
 1018 default model parameters and spin-up settings do not produce this; augmented warming or incoming radiation fluxes need to
 1019 be introduced to the ERA climatology to produce temperate firm at this time. It is possible that strong melt seasons in the
 1020 early 1960s created temporary temperate conditions in the upper firm column. Alternatively, the surface energy balance and
 1021 firm hydrological models may underestimate the amount of melting and meltwater infiltration. The one firm conclusion is
 1022 that the climatological and glaciological conditions on the upper Kaskawulsh Glacier are very close to the tipping point
 1023 between polythermal and temperate conditions. A slight nudge to either side of the reference model settings can give either
 1024 persistently sub-zero or persistently thawed conditions in the deep firm at this site (Figures 7 and S1).

1025

1026 The presence of the deep PFA in 2018 indicates that it is currently temperate, despite mean annual air temperatures of about
 1027 -11°C . Meltwater refreezing releases enough latent heat to bring the firm to 0°C . All model simulations concur on this,
 1028 although the long-term evolution is uncertain. We don’t know the fate of the water that drains through the firm, but the
 1029 reference model predicts a total drainage of 1.13 m w.e. over the 55-year simulation, most of this over the last decade. Some
 1030 of this is retained within the PFA, but some can be expected to run off. The water in the PFA on Kaskawulsh Glacier is
 1031 likely to be flowing, redistributing mass. The drill site was located high in the glacier’s accumulation zone, with a gently
 1032 sloping surface ($< 0.6^{\circ}$) resulting in a subtle hydraulic gradient. We likely drilled into the top of the water table of the PFA.
 1033 There may be downslope flow along the firm-ice interface, as well as possible Darcian flow within the PFA itself (e.g.,
 1034 Christianson et al., 2015).

1035

1036 The liquid-phase meltwater retention on Kaskawulsh is similar to the PFAs found in the high-accumulation areas of southern
 1037 Greenland and Svalbard (e.g., Miège et al., 2016; Christianson et al., 2015), and different than the water-saturated layers
 1038 commonly found on temperate glaciers. PFAs that have been studied on temperate mountain glaciers typically have a
 1039 saturated layer close to the surface (for example, 5 m below the surface at Storglaciären), have active discharge and recharge
 1040 processes (Fountain and Walder, 1998; Schneider, 1999; Glazyrin et al., 1977), and appear to experience seasonal drainage
 1041 over the winter months (Fountain, 1989, 1996; Jansson et al., 2003), likely due to high hydraulic gradients. Active water
 1042 flow in the firm has been observed in 19-m and 25-m pits at Abramov Glacier (Glazyrin et al., 1977), as well as Austfonna
 1043 ice cap in 1985 at 7 m depth where they also found sub-horizontal melt channels at 7, 15, and 30 m (Zagorodnov et al.,
 1044 2006). In 2012, “water-saturated” firm was found at 40-m depth in an ice core from Mt. Waddington, British Columbia (Neff
 1045 et al., 2012). However, they reported no significant alteration of chemistry from the melt above this layer and no additional

- Luke Copland 1/25/2021 3:15 PM
- Deleted:** ry
- Luke Copland 1/25/2021 3:15 PM
- Deleted:** Material
- Luke Copland 1/25/2021 3:15 PM
- Deleted:** just
- Luke Copland 1/25/2021 3:16 PM
- Deleted:** very
- Naomi Ochwat 1/28/2021 10:21 PM
- Deleted:** firm aquifer
- Shawn Marshall 1/19/2021 9:58 AM
- Deleted:** ... [39]
- Shawn Marshall 1/6/2021 2:06 PM
- Moved up [3]:** The firm model predicted the development of wet, temperate conditions in the deep firm following the 2013 melt season, al... [40]
- Naomi Ochwat 1/28/2021 10:21 PM
- Deleted:** firm aquifer
- Naomi Ochwat 1/28/2021 10:21 PM
- Deleted:** firm aquifer
- Shawn Marshall 1/6/2021 7:04 PM
- Deleted:** *
- Naomi Ochwat 1/28/2021 10:21 PM
- Deleted:** firm aquifer
- Shawn Marshall 1/6/2021 6:53 PM
- Deleted:** down slope
- Naomi Ochwat 1/28/2021 10:21 PM
- Deleted:** firm aquifer
- Shawn Marshall 1/6/2021 6:54 PM
- Deleted:** It may also enter the englacial ... [41]
- Naomi Ochwat 1/28/2021 10:21 PM
- Deleted:** firm aquifer
- Naomi Ochwat 1/28/2021 7:15 PM
- Deleted:** Firm aquifers
- Shawn Marshall 1/6/2021 6:59 PM
- Deleted:** slope
- Shawn Marshall 1/19/2021 9:42 AM
- Deleted:** In 1977 atop Abramov glacier
- Shawn Marshall 1/19/2021 9:43 AM
- Deleted:**
- Shawn Marshall 1/19/2021 9:43 AM
- Deleted:**
- Naomi Ochwat 1/27/2021 10:26 PM
- Deleted:**
- Shawn Marshall 1/19/2021 9:43 AM
- Deleted:** showed active water flow through the firm

1093 analysis of this layer was discussed (Neff et al., 2012). In 2015, a PFA was found on Holtedahlfonna icefield in Northwest
1094 Svalbard (Christianson et al., 2015), and in 2019 a PFA was investigated at Lomonosovfonna ice cap approximately 100 km
1095 to the southeast (Hawrylak and Nilsson, 2019).

1096
1097 According to Kuipers Munneke et al. (2014), PFA formation in Greenland is contingent upon a high annual snow
1098 accumulation, which helps to insulate the underlying firn from the winter cold wave. Mean annual temperatures in
1099 Greenland are well below 0°C and PFAs require latent heat release from meltwater refreezing, to warm the snow and firn to
1100 0°C, along with meltwater penetration to depths of at least 10 m, to evade the winter cold wave (Kuipers Munneke et al.,
1101 2014). The firn modelling suggests that meltwater penetration to depths of 10 m is rare at Kaskawulsh Glacier, but can occur
1102 in strong melt seasons. Based on our measurements and earlier reports from the IRRP (Wood, 1963; Grew and Mellor,
1103 1966), the estimated accumulation rate at our study site is 1.8 m w.e. yr⁻¹. This is similar to reported accumulation rates
1104 where PFAs have been identified in southeastern Greenland (e.g., Miège et al., 2016). Melt rates at southeast Greenland PFA
1105 locations are also comparable to those on the upper Kaskawulsh. Miège et al. (2016) report 0.73 m w.e. yr⁻¹ over the time
1106 period 1979-2014, while Miller et al. (2020) estimate annual melt rates from 0.24-0.50 m w.e. yr⁻¹ in a PFA field study at
1107 1700 m elevation in the Helheim Glacier catchment. Modelled melt rates on the upper Kaskawulsh Glacier are estimated at
1108 0.52±0.27 m w.e. yr⁻¹ from 1965-2019 (Table 2). Recent (2005-2017) Kaskawulsh melt rates increased to 0.72 ± 0.38 m
1109 w.e. yr⁻¹, similar to the long-term estimate of Miège et al. (2016) in southeast Greenland, and perhaps close to the threshold
1110 for PFA formation and recharge.

1111 5.3 Implications for geodetic mass balance

1112 The solid and liquid phase storage mechanisms in the Kaskawulsh Glacier firn layer have different implications for the mass
1113 balance of the glacier. Liquid water is commonly found in the temperate firn of low- and mid- latitude mountain glaciers and
1114 has played an important role in meltwater storage and glacier hydrology (Fountain and Walder, 1989; Schneider, 1999).
1115 Depending on the melt, PFA thickness, and temperature of the firn, the storage of liquid water at the firn-ice interface delays
1116 runoff from hours to weeks or longer (Jansson et al., 2003). This melt can account for as much as 64% of internal
1117 accumulation, as found in Alaska and Sweden (Trabant and Mayo, 1985; Schneider and Jansson, 2004).

1118
1119 The effects of meltwater storage through refreezing or liquid retention on high mountain glaciers complicate mass balance
1120 measurements. The climate reanalysis suggests that these effects are increasing as the climate is warming. Geodetic mass
1121 balance measurements are compromised by climate change-induced densification that causes surface lowering of the
1122 accumulation zone (Reeh, 2008; Huss, 2013). Mass balance studies in Greenland indicate that changing melt regimes,
1123 meltwater refreezing, and the unknown density and pore capacity of snow and firn pose significant uncertainties when
1124 modelling the surface mass balance of large ice sheets (Lenaerts et al., 2019). Meltwater retention as porewater or refrozen
1125 ice will delay surface runoff, dependent on the water storage characteristics of firn (e.g., pore space availability, water at

Naomi Ochwat 12/19/2020 7:00 AM

Deleted: Apart from these studies, there have been no other published reports of PFAs on mountain glaciers (Christianson et al., 2015).

Shawn Marshall 1/6/2021 7:02 PM

Deleted: -

Shawn Marshall 1/6/2021 7:02 PM

Deleted: -

Naomi Ochwat 1/28/2021 10:21 PM

Deleted: firn aquifer...FA formation in G... [42]

Shawn Marshall 1/19/2021 9:44 AM

Deleted: : (i)...latent heat release from mc... [43]

Shawn Marshall 1/28/2021 12:23 PM

Formatted [44]

Shawn Marshall 1/28/2021 11:54 AM

Deleted: and Miller et al., (2020) report values from 31 - 156 cm a year... This is significant... [45]

Naomi Ochwat 1/28/2021 10:21 PM

Deleted: firn aquifer

Shawn Marshall 1/28/2021 12:25 PM

Deleted: The firn modeling suggests meltwater penetration to depths of 10 m or more and is also evident from the field observation of liquid water being expelled from the core. It appears that firn aquifer formation on Kaskawulsh Glacier is similar to that in Greenland

Naomi Ochwat 1/28/2021 10:21 PM

Deleted: firn aquifer...FA thickness, and... [46]

Shawn Marshall 1/28/2021 10:58 AM

Deleted: the subsequent meltwater storage... [47]

interstitial grain boundaries) (Fountain and Walder, 1989; Schneider, 1999). If ice layers become too extensive or thick, they can form an 'ice slab,' a thick impermeable barrier that leads to enhanced surface runoff (MacFerrin et al., 2019). The thickness of ice layers that prevents percolation is not well understood. For example, in Greenland 12-cm thick ice layers were still permeable (Samimi et al., 2020) whereas Bell et al. (2008) reported that a 1-2 cm ice layer prevented percolation at the Devon Ice Cap, Canada. These phenomena and effects are not limited to Greenland and the high Arctic. This study demonstrates that Kaskawulsh Glacier also experiences meltwater storage in the form of ice layers and liquid water retention (as a PFA), with potentially significant recent changes in firm structure and meltwater retention capacity. The increases in firm density and ice content found on Kaskawulsh Glacier appear to be similar to other high-accumulation Arctic regions (Pohjola et al., 2002; De La Peña et al., 2015; Bezeau et al., 2013).

The surface energy balance model is not observationally constrained at this site, so we don't have quantitative confidence in the modelled mass balance and melt rates, but the reconstructed trends indicate a ~70% increase in summer meltwater production at this site since the 1960s, leading to increased rates of refreezing and also the onset of meltwater runoff in recent years. Melt totals are well less than the annual accumulation (~1.8 m w.e.), so the site remains within the accumulation area of the glacier, with most of the meltwater refreezing. Increases in annual meltwater refreezing drive increased ice content and densification at this site. The modelling suggests a ~5% increase in firm density since the 1960s and a doubling of the ice content, from 1.1 to 2.3 m over the full 35-m snow/firm column. Recent increases in summer melting would also contribute to surface drawdown, as well as mass loss. Within the model, 96% of total meltwater refreezes over the 55-year simulation, but this is reduced to 86% for the period represented by the firm core, 2005-2017. The remaining 27% drains to the deep firm through this period, where it is either retained within the PFA or it may drain from the system. A total of ~1.3 m w.e. 'runs off' through the period 2005-2017. In the model, this drains through the bottom layer and leaves the system; in reality, this water may drain through lateral transport in the PFA or at the ice-firm interface.

The modelled 2018 firm core has an ice content of 2.6 m, compared to a total ice content of 2.33 ± 0.26 m measured in Core 1. The modelled ice content is a completely independent estimate and is in reasonable agreement with the firm core, giving some confidence in the modelled refreezing, but it is about 15% in excess of the observations. This suggests that the model may slightly over-estimate the melt or the meltwater infiltration. However, that inference is not consistent with the apparent cold bias in the model spin-up. Alternatively, firm in the model may be too cold through much of the simulation, causing an overestimate of the modelled meltwater refreezing and retention capacity. If this is the case, runoff (summer mass losses) from the site will be higher than our estimates, with negative implications for Kaskawulsh Glacier mass balance.

The accumulation zone of Kaskawulsh Glacier is estimated to have experienced a minimum of 0.73 ± 0.23 m of surface lowering due to internal refreezing over the period represented by Core 1, which we estimate to be 12.5 years, or 0.06 ± 0.02 m yr⁻¹ from 2005-2017. This estimate of thinning is likely low, because neither the meltwater retention due to the infiltration

- Shawn Marshall 1/6/2021 7:13 PM
Deleted: varies and depends on the local climate and conditions of the firm
- Shawn Marshall 1/28/2021 11:00 AM
Deleted: . These features in and of themselves are not unique to glaciers
- Shawn Marshall 1/28/2021 11:03 AM
Deleted: but their change here is
- Shawn Marshall 1/28/2021 11:01 AM
Deleted: firm stratigraphy and change in densification
- Shawn Marshall 1/28/2021 10:56 AM
Deleted: is
- Shawn Marshall 1/28/2021 10:56 AM
Deleted: high
- Shawn Marshall 1/6/2021 7:14 PM
Deleted: T
- Shawn Marshall 1/6/2021 7:15 PM
Deleted: melt rates
- Shawn Marshall 1/6/2021 7:15 PM
Deleted: doubling
- Shawn Marshall 1/6/2021 7:15 PM
Deleted: of
- Shawn Marshall 1/16/2021 12:12 PM
Deleted: always remain
- Shawn Marshall 1/6/2021 7:17 PM
Deleted: in recent years would
- Shawn Marshall 1/28/2021 10:38 AM
Deleted: mass loss due to deep meltwater percolation
- Shawn Marshall 1/6/2021 7:36 PM
Deleted: ('runoff')
- Shawn Marshall 1/28/2021 10:37 AM
Deleted: , particularly since 2013 when runoff started to increase
- Naomi Ochwat 1/28/2021 8:47 PM
Deleted: The remaining 14%, which equals ~1.3 m w.e., drains to the deep firm through this period, where it is either retained within the firm aquifer or it may drain from the system. Within the model ... [48]
- Shawn Marshall 1/7/2021 9:43 AM
Formatted: Font:6 pt
- Shawn Marshall 1/7/2021 9:42 AM
Formatted: Font:6 pt
- Naomi Ochwat 12/19/2020 7:04 AM
Deleted: a conservative estimate
- Shawn Marshall 1/7/2021 9:42 AM
Deleted: a lower estimate

1258 ice nor the presence of the PFA is included in this estimate. In previous measurements of surface elevation changes on
1259 Kaskawulsh Glacier, Foy et al. (2011) found that the accumulation zone thinned by an average of 0.04-0.11 m yr⁻¹ from
1260 1977-2007, with a total thinning of 1-3 m over this period. Larsen et al. (2015) reported mean elevation losses of 0-1 m yr⁻¹
1261 towards the head of the glacier from 1995-2000. The thinning signal due to meltwater percolation and refreezing is within
1262 the estimates of Foy et al. (2011) and Larsen et al. (2015), suggesting that some or all of the reported lowering could be due
1263 to mass redistribution and not mass loss. The density of the firm has increased from 1964-2018 due to meltwater percolation
1264 and refreezing. It is therefore likely that the surface has lowered since 1964 because of this increased densification.

1265 6 Conclusion

1266 The upper accumulation zone of Kaskawulsh Glacier firm has undergone significant changes since 1964. The firm has
1267 become warmer, denser, and more ice-rich since 1964. The firm now contains a PFA, which has likely developed over the
1268 past decade. The mean density of the first 32 m of firm (4.2 to 36.2 m below the surface) was 698 ± 5 kg m⁻³, and firm
1269 densification due to meltwater refreezing into ice layers over the last ~12.5 years (2005-2017) is responsible for an estimated
1270 surface lowering of 0.73 ± 0.23 m. The PFA may be a recent feature, attributed to increased summer melting, meltwater
1271 infiltration, and firm warming from the associated latent heat release. Our study illustrates a high elevation accumulation area
1272 that is changing in response to climate-driven surface warming and provides density information required for geodetic mass
1273 balance calculations.

1274
1275 This study has utilized historical density data in order to assess the changes in densification due to meltwater percolation and
1276 refreezing since 1964. The firm of Kaskawulsh Glacier has become up to 15% denser due to the increased amount of ice
1277 layers and melt-affected firm. The Kaskawulsh Glacier PFA needs to be more widely studied. The spatial extent and depth of
1278 the aquifer is not yet known. Ground penetrating radar measurements may provide a method to investigate the spatial extent
1279 of the feature. Use of an electrothermal drill that can drill through water-saturated firm may allow estimations of the depth of
1280 the firm aquifer, as well as subsequent studies on the potential flow of the water within the aquifer. This region will likely
1281 continue to experience increasing amounts of surface melt and refreezing within the snowpack and firm, so there is urgency
1282 to obtain climate records from this region.

1283
1284 *Data availability.* Raw density data is available by contacting the corresponding author.

1285
1286 *Author contribution.* NO and AC collected field data. AC ran ion analyses, supervised the field campaign and helped with
1287 figures. SM contributed to the design and funding of the study and was responsible for the firm modelling. BM and SM
1288 provided supervision during the project. LC provided weather station data and contributed to the collection and interpretation
1289 of data. NO analysed the data and wrote the manuscript, to which all co-authors contributed.

Naomi Ochwat 1/28/2021 10:21 PM

Deleted: firm aquifer

Naomi Ochwat 1/29/2021 12:17 PM

Deleted: The thinning signal due to meltwater percolation and refreezing is within the estimates of Foy et al.'s (2011) and Larsen et al. (2015)'s estimates, suggesting that some or all of the reported lowering could be due to mass redistribution and not mass loss. The density of the firm has increased from 1964-2018 due to meltwater percolation and refreezing, and liquid water retention processes cause the surface to lower. It is therefore likely that the surface has lowered since 1964 because of this increased densification.

Naomi Ochwat 1/29/2021 12:17 PM

Formatted: English (US)

Naomi Ochwat 1/28/2021 10:21 PM

Deleted: perennial firm aquifer

Naomi Ochwat 1/28/2021 7:16 PM

Deleted: (PFA),

Shawn Marshall 1/6/2021 7:47 PM

Deleted: is

Shawn Marshall 1/6/2021 7:48 PM

Deleted: that is

Shawn Marshall 1/6/2021 7:48 PM

Deleted: the

Shawn Marshall 1/6/2021 7:48 PM

Deleted: warming climate and increased melt

Shawn Marshall 1/6/2021 7:50 PM

Deleted: 4.

Shawn Marshall 1/6/2021 7:50 PM

Deleted: The historical changes also indicate that the firm temperature has increased by an average of 1.7°C with complete removal of the winter cold wave by July, as reported in 2006. ... [49]

Shawn Marshall 1/19/2021 11:15 AM

Deleted: , conception,

Shawn Marshall 1/6/2021 9:07 AM

Deleted: SM

Shawn Marshall 1/6/2021 9:07 AM

Deleted: BM

Shawn Marshall 1/19/2021 11:15 AM

Deleted: ,

Shawn Marshall 1/19/2021 11:16 AM

Deleted: . NO

1319
1320 *Competing interests.* The authors declare no competing interests.
1321
1322 *Acknowledgements.* This work was part of a Polar Knowledge Canada Grant in support of Cryosphere-Climate Monitoring at
1323 Kluane Lake Research Station, Yukon Territory. We acknowledge the Natural Sciences and Engineering Research Council
1324 (NSERC) of Canada for additional financial support. We thank Parks Canada for permission to conduct this research in
1325 Kluane National Park, under research and collection permit KLU-2018-28117. We are grateful for the field crew Étienne
1326 Gros and Peter Moraal, Icefield Instruments Inc., for assistance with coring, and members of the University of Ottawa
1327 Glaciology and Northern Field Research classes, particularly Jean Bjornson, for assistance with the snow pit measurements.
1328 The Arctic Institute of North America, Kluane Lake Research Station, and Icefield Discovery supported fieldwork logistics.
1329 We thank Kristina Miller, University of Calgary, for field support and countless glaciological discussions, Shad O’Neel and
1330 Louis Sass of the U.S. Geological Survey for sharing firn density data from Alaska, Christian Zdanowicz, Uppsala
1331 University, for sharing his 2004-2011 snow depth data from the [upper Hubbard Glacier](#), and [Eduard Khachatryan](#) for
1332 [translating the Glazyrin et al. \(1977\) paper](#).

1333 **References**

- 1334 Bader, H.: Sorge’s law of densification of snow on high polar glaciers, *J. Glaciol.*, 2, 319–323, 1954.
- 1335 Bell, C., Mair, D., Burgess, D., Sharp, M., Demuth, M., Cawkwell, F., Bingham, R. and Wadham, J.: Spatial and temporal
1336 variability in the snowpack of a High Arctic ice cap: implications for mass-change measurements. *Ann. Glaciol.* 48, 159-
1337 170, 2008.
- 1338 Berthier, E., Schiefer, E., Clarke, G. K. C., Menounos, B. and Rémy, F: Contribution of Alaskan glaciers to sea-level rise
1339 derived from satellite imagery. *Nat. Geosci.* 3, 92–95, 2010.
- 1340 Bezeau, P., Sharp, M., Burgess, D. and Gascon, G: Firn profile changes in response to extreme 21st-century melting at
1341 Devon Ice Cap, Nunavut, Canada. *J. Glaciol.* 59, 981–991, 2013.
- 1342 Christianson, K., Kohler, J., Alley, R. B., Nuth, C. and Van Pelt, W. J. J.: Dynamic perennial firn aquifer on an Arctic
1343 glacier. *Geophys. Res. Lett.* 42, 1418–1426, 2015.
- 1344 Cogley, J.G.: Geodetic and direct mass-balance measurements: comparison and joint analysis. *Ann. Glaciol.*, 50(50), 96-100,
1345 2009.
- 1346 Coleou, C., and Lesaffre, B.: Irreducible water saturation in snow: experimental results in a cold laboratory. *Ann.*
1347 *Glaciol.*, 26, 64–68, <https://doi.org/10.3189/1998AoG26-1-64-68>, 1998.
- 1348 Cuffey, K. M., and Paterson, W.: *The Physics of Glaciers* (4th ed.). Boston,; Elsevier. 1-683. 2010.

Shawn Marshall 1/19/2021 11:16 AM

Deleted: and

Shawn Marshall 1/19/2021 11:16 AM

Deleted: Divide site.

Shawn Marshall 1/19/2021 11:16 AM

Deleted: .

- 1352| De La Peña, S, I. M. Howat, P.W. Nienow, M. R. van den Broeke, E. Mosley-Thompson, S. F. Price, D. Mair, B. Noël, and
 1353| A. J. Sole.: Changes in the firm structure of the western Greenland Ice Sheet caused by recent warming. *The Cryosphere*, 9,
 1354| 1203–1211, 2015.
- 1355| Ebrahimi, S. and Marshall, S. J.: Surface energy balance sensitivity to meteorological variability on Haig Glacier, Canadian
 1356| Rocky Mountains, *The Cryosphere*, 10, 2799–2819, <https://doi.org/10.5194/tc-10-2799-2016>, 2016.
- 1357| Fountain, A. G.: The storage of water in, and hydraulic characteristics of, the firm of South Cascade Glacier, Washington
 1358| State, USA. *Ann. Glaciol.*, 13, 69–75. 1989.
- 1359| Fountain, A. G.: Effect of Snow and Firn Hydrology on the Physical and Chemical Characteristics of Glacial Runoff.
 1360| *Hydrol. Process.* 10, 509–521, 1996.
- 1361| Fountain, A. G. and Walder, J. S.: Water flow through temperate glaciers. *Rev. Geophys.*, 36, 299–328. 1998.
- 1362| Foy, N., Copland, L., Zdanowicz, C., Demuth, and M., Hopkinson, C.: Recent volume and area changes of Kaskawulsh
 1363| Glacier, Yukon, Canada. *J. Glaciol.*, 57, 515–525, <https://doi.org/10.3189/002214311796905596>, 2011.
- 1364| Gascon, G., Sharp, M., Burgess, D., Bezeau, P. and Bush, A. B. G.: Changes in accumulation-area firn stratigraphy and
 1365| meltwater flow during a period of climate warming: Devon Ice Cap, Nunavut, Canada. *J. Geophys. Res. Earth Surf.* 118,
 1366| 2380–2391, 2013.
- 1367| Grew, E., and Mellor, M.: High snowfields of the St. Elias Mountains, Yukon Territory, Canada. Hanover, N.H. U.S. Army
 1368| Materiel Command, Cold Regions Research & Engineering Laboratory Technical Report, 177, 1-26, 1966.
- 1369| [Glazyrin G.E., Glazyrina E.L., Kislov B.V. and Pertzinger F.I. Water level regime in deep firn pits on Abramov glacier \[in
 1370| Russian\], volume 45. Gidrometeoizdat, 2017.](#)
- 1371| Harper, J., Humphrey, N., Pfeffer, W. T., Brown, J., and Fettweis, X.: Greenland ice-sheet contribution to sea-level rise
 1372| buffered by meltwater storage in firn. *Nature*, 491, 240–243, 2012.
- 1373| Harper, J., Humphrey, N., Pfeffer, T. and Brown, J.: Firn Stratigraphy and Temperature to 10 m Depth in the Percolation
 1374| Zone of Western Greenland, 2007 – 2009. Institute of Arctic and Alpine Research, University of Colorado, Occasional Paper
 1375| 60, 2011.
- 1376| Hawrylak, M., and Nilsson, E.: Spatial and Temporal Variations in a Perennial Firn Aquifer on Lomonosovfonna, Svalbard.
 1377| Uppsala University Independent Project, 2019. <http://www.diva-portal.se/smash/get/diva2:1319193/FULLTEXT01.pdf>.
- 1378| Hersbach, H., Bell, B., Berrisford, P. et al.: The ERA5 global reanalysis. *Quarterly Journal of the Royal Meteorological
 1379| Society*, <https://doi.org/10.1002/qj.3803>, 2020.
- 1380| Holdsworth, G.: An Examination and Analysis of the Formation of Transverse Crevasses, Kaskawulsh Glacier, Yukon
 1381| Territory, Canada. Institute of Polar Studies, 16, 1965.
- 1382| Humphrey, N. F., Harper, J. T., and Pfeffer, W. T.: Thermal tracking of meltwater retention in Greenland’s accumulation
 1383| area. *J. Geophys. Res.*, 117, F01010, <https://doi.org/10.1029/2011JF002083>, 2012.
- 1384| Huss, M.: Density assumptions for converting geodetic glacier volume change to mass change, *The Cryosphere*, 7, 219–244.
 1385| 2013.

Naomi Ochwat 1/17/2021 7:25 PM
 Formatted: English (US)

1386 Jansson, P., Hock, R. and Schneider, T.: The concept of glacier storage: A review. *J. Hydrol.*, 282, 116–129, 2003.

1387 Koenig, L. S., Miège, C., Forster, R. R. and Brucker, L.: Initial in situ measurements of perennial meltwater storage in the
1388 Greenland firn aquifer. *Geophys. Res. Lett.* 41, 81–85, 2014.

1389 Koerner, R. M.: Devon Island Ice Cap: Core Stratigraphy and Paleoclimate. *Science*, 146, 347–353. 1977.

1390 [Kuipers Munneke, P. K., Ligtenberg, S. R. M., Van Den Broeke, M. R., Van Angelen, J. H. and Forster, R. R.: Explaining
1391 the presence of perennial liquid water bodies in the firn of the Greenland Ice Sheet. *Geophys. Res. Lett.* 41, 476–483, 2014.](#)

1392 Larsen, C. F., Burgess, E., Arendt, A. A., O'Neel, S., Johnson, A. J., and Kienholz, C.: Surface melt dominates Alaska
1393 glacier mass balance. *Geophys. Res. Lett.* 42, 5902–5908. <https://doi.org/10.1002/2015GL064349>, 2015.

1394 Lenaerts, J. T. M., Medley, B., van den Broeke, M. R. and Wouters, B.: Observing and Modeling Ice Sheet Surface Mass
1395 Balance. *Rev. Geophys.* 57, 376–420, <https://doi.org/10.1029/2018RG000622>, 2019.

1396 Ligtenberg, S. R. M., Helsen, M. M., and van den Broeke, M. R.: An improved semi-empirical model for the densification of
1397 Antarctic firn, *The Cryosphere*, 5, 809–819, doi:10.5194/tc-5-809-2011, 2011.

1398 [Machguth, H., MacFerrin, M., van As, D., Jason E. Box, Charalamos Charalampidis, William Colgan, Robert S. Fausto,
1399 Harro AJ Meijer, Ellen Mosley-Thompson, and Roderik SW van de Wal.: Greenland meltwater storage in firn limited by
1400 near-surface ice formation. *Nature Clim Change*. 6, 390–393. <https://doi.org/10.1038/nclimate2899>, 2016.](#)

1401 MacFerrin, M. Machguth H, van As, D. C. Charalampidis, C., C. M. Stevens, C.M., Heilig, A., Vandecrux, B., P. L. Langen,
1402 P. L., Mottram, R., Fettweis, X., van den Broeke, M. R., Pfeffer, W. T., M. S. Moussavi, M. S., and Abdalati. W.: Rapid
1403 expansion of Greenland's low-permeability ice slabs. *Nature*, 573, 403–407, 2019.

1404 Marcus, M. G. and Ragle, R. H. Snow accumulation in the Icefield Ranges, St. Elias Mountains, Yukon. *Arctic and Alpine
1405 Research*, 2(4), 277-292, 1970.

1406 Miège, C., Forster, R., Brucker, L., Koenig, L., Solomon, D.K., Paden, J. D., Box, J. E., Burges, E. W., Miller, J. Z.,
1407 McNerney, L., Brautigam, N., Fausto, R. S., and Gogineni, S.: Spatial extent and temporal variability of Greenland firn
1408 aquifers detected by ground and airborne radars. *J. Geophys. Res. Earth Surf*, 121, 2381–2398, _
1409 <https://doi.org/10.1002/2016JF003869>, 2016.

1410 [Miller, O., Solomon, D. K., Miège, C., Koenig, L., Forster, R., Schmerr, N. et al. : Hydrology of a perennial firn aquifer in
1411 southeast Greenland: An overview driven by field data. *Water Resources Research*, 56, e2019WR026348. \[https://doi.org/
1412 10.1029/2019WR026348\]\(https://doi.org/10.1029/2019WR026348\), 2020.](#)

1413 [Moholdt, G., Nuth, C., Hagen, J. O. and Kohler, J.: Recent elevation changes of Svalbard glaciers derived from ICESat laser
1414 altimetry. *Remote Sens. Environ.*, 114, 2756–2767, 2010a.](#)

1415 [Moholdt, G., Hagen, J. O., Eiken, T. and Schuler, T. V.: Geometric changes and mass balance of the Austfonna ice cap,
1416 Svalbard. *The Cryosphere*, 4, 21–34, 2010b.](#)

1417

1418

1419

1420 [Neff, P. D., Steig, Eric J., Clark, Douglas H., McConnell, Joseph R., Pettit, Erin C., and Menounos, Brian.: Ice-core net snow
1421 accumulation and seasonal snow chemistry at a temperate-glacier site: Mount Waddington, southwest British Columbia,
1422 Canada. *J. Glaciol.* 58\(212\), 1165-1175. <https://doi.org/10.3189/2012JoG12J078>, 2012.](#)

Naomi Ochwat 12/19/2020 7:12 AM
Deleted: Machguth, H., Eisen, O., Paul, F. and Hoelzle, M.: Strong spatial variability of snow accumulation observed with helicopter-borne GPR on two adjacent Alpine glaciers. *Geophys. Res. Lett.* 33, 1–5, 2016.

Naomi Ochwat 1/28/2021 10:19 PM
Formatted: Justified

Shawn Marshall 1/28/2021 11:58 AM
Deleted: &

Shawn Marshall 1/28/2021 11:58 AM
Deleted: .

Shawn Marshall 1/28/2021 11:59 AM
Formatted: Font:(Default) +Theme Body, Font color: Text 1

Naomi Ochwat 1/28/2021 10:19 PM
Formatted: Space After: 0 pt, Pattern: Clear (White)

Shawn Marshall 1/28/2021 12:10 PM
Formatted: Font:(Default) +Theme Body, 10 pt, English (CAN)

Shawn Marshall 1/28/2021 12:10 PM
Formatted: English (CAN)

Shawn Marshall 1/28/2021 12:10 PM
Formatted: Font:(Default) +Theme Body, 10 pt, English (CAN)

Shawn Marshall 1/28/2021 12:10 PM
Formatted: Font:(Default) +Theme Body, 10 pt

Shawn Marshall 1/28/2021 12:10 PM
Formatted: Font:(Default) +Theme Body, 10 pt

Shawn Marshall 1/28/2021 12:10 PM
Formatted: ... [50]

Shawn Marshall 1/28/2021 12:10 PM
Formatted: ... [51]

Shawn Marshall 1/28/2021 12:10 PM
Formatted: ... [52]

Naomi Ochwat 1/28/2021 10:19 PM
Formatted: ... [53]

Naomi Ochwat 1/28/2021 7:34 PM
Formatted: ... [54]

Naomi Ochwat 1/28/2021 10:19 PM
Formatted: Space After: 0 pt

Shawn Marshall 1/28/2021 11:57 AM
Deleted: Miller, O., Solomon, D. K., Miège ... [55]

Naomi Ochwat 1/17/2021 8:52 PM
Deleted: Munneke, P. K., Ligtenberg, S. R. ... [56]

1445 Noël, B., van de Berg, W.J., Lhermitte, S., Wouters, B., Schaffer, N. and van den Broeke, M.R., 2018. Six decades of glacial
1446 mass loss in the Canadian Arctic Archipelago. *J. Geophys. Res. Earth Surf.*, 123(6), 1430-1449.
1447 <https://doi.org/10.1029/2017JF004304>, 2018.

1448 Noël, B., Jakobs, C.L., van Pelt, W.J.J., Lhermitte, S., Wouters, B., Kohler, J., Hagen, J.O., Luks, B., Reijmer, C.H., Van de
1449 Berg, W.J. and van den Broeke, M.R.: Low elevation of Svalbard glaciers drives high mass loss variability. *Nat Commun.*
1450 11(1), 1-8. <https://doi.org/10.1038/s41467-020-18356-1> 2020.

1451 Parry, V., Nienow, P., Mair, D., Scott, J., Hubbard, B., Steffen, K., and Wingham, D.: Investigations of meltwater refreezing
1452 and density variations in the snowpack and firn within the percolation zone of the Greenland ice sheet. *Ann. Glaciol.* 61–68.
1453 2007.

1454 Pohjola, V. A., Moore, J. C., Isaksson, E., Jauhiainen, T., van de Wal, R. S. W., Martma, T., Meijer, H. A. J., and Vaikmäe,
1455 R.: Effect of periodic melting on geochemical and isotopic signals in an ice core from Lomonosovfonna, Svalbard. *J.*
1456 *Geophys. Res.*, 107, 4036, 2002.

1457 Poli, P., Hersbach, H., Dee, D. P. and 12 others.: ERA-20C: An atmospheric reanalysis of the 20th century. *J. Climate*, 29
1458 (11), 4083-407, <https://doi.org/10.1175/JCLI-D-15-0556.1>, 2016.

1459 Reeh, N.: A nonsteady-state firn-densification model for the percolation zone of a glacier, *J. Geophys. Res.*, 113,
1460 F03023, doi:10.1029/2007JF000746, 2008.

1461 Rohatgi, A., WebPlotDigitizer. Version 4.3. 2020. <https://automeris.io/WebPlotDigitizer>

1462 Samimi, S. and Marshall, S. J.: Diurnal cycles of meltwater percolation, refreezing, and drainage in the supraglacial
1463 snowpack of Haig Glacier, Canadian Rocky Mountains. *Front. Earth Sci.* 5, 1–15. <https://doi.org/10.3389/feart.2017.00006>,
1464 2017.

1465 Samimi, S., Marshall, S. J., and MacFerrin, M.: Meltwater penetration through temperate ice layers in the percolation zone at
1466 DYE-2, Greenland Ice Sheet. *Geophys. Res. Lett.*, 47, e2020GL089211. 2020.

1467 Schaffer, N., Copland, L., Zdanowicz, C., Burgess, D., & Nilsson, J.: Revised estimates of recent mass loss rates for Penny
1468 Ice Cap, Baffin Island, based on 2005–2014 elevation changes modified for firn densification *J. Geophys. Res. Earth Surf.*
1469 125, e2019JF005440. 2020. <https://doi.org/10.1029/2019JF005440>

1470 Schneider, T.: Water movement in the firn of Storglaciären. *J. Glaciol.* 45, 286–294, 1999.

1471 Schneider, T. & Jansson, P. Internal accumulation in firn and its significance for the mass balance of Storglaciären, Sweden.
1472 *J. Glaciol.* 50, 25–34, 2004.

1473 Sorge, E. (1935). *Glaziologische Untersuchungen in Eismitte. Wissenschaftliche Ergebnisse der Deutschen Gronland-*
1474 *Expedition Alfred-Wegener 1929 und 1930-1931.* 3, 270. in: K. Wegener, im Auftrag der Notgemeinschaft der Deutschen
1475 *Wissenschaft (Ed.), Band III. Glaziologie, 1935.*

1476 Trabant, D. C. and Mayo, L. R.: Estimation and effects of internal accumulation on five glaciers in Alaska. *Ann. Glaciol.*, 6,
1477 113–117, 1985.

1479 van As, D., Box, J. E., and Fausto, R. S.: Challenges of Quantifying Meltwater Retention in Snow and Firn: An Expert
1480 Elicitation., *Front. Earth Sci.* 4(101), <https://doi.org/10.3389/feart.2016.00101>, 2016.

- Naomi Ochwat 1/28/2021 7:39 PM
Formatted: Font:Not Italic
- Naomi Ochwat 1/28/2021 7:40 PM
Formatted: Font:Not Italic
- Naomi Ochwat 1/28/2021 7:36 PM
Formatted: Font:Not Italic
- Naomi Ochwat 1/28/2021 7:36 PM
Formatted: Font:Not Italic
- Unknown
Field Code Changed
- Shawn Marshall 1/28/2021 12:15 PM
Deleted: Cycles
- Shawn Marshall 1/28/2021 12:15 PM
Deleted: Meltwater
- Shawn Marshall 1/28/2021 12:15 PM
Deleted: Percolation
- Shawn Marshall 1/28/2021 12:15 PM
Deleted: Refreezing
- Shawn Marshall 1/28/2021 12:15 PM
Deleted: Drainage
- Shawn Marshall 1/28/2021 12:15 PM
Deleted: Supraglacial
- Shawn Marshall 1/28/2021 12:15 PM
Deleted: Snowpack
- Naomi Ochwat 1/28/2021 10:19 PM
Formatted: Justified
- Naomi Ochwat 1/28/2021 7:30 PM
Formatted: Font:Not Italic
- Naomi Ochwat 1/28/2021 10:07 PM
Formatted: Font:Not Italic
- Naomi Ochwat 1/28/2021 7:30 PM
Formatted: Font:Italic
- Naomi Ochwat 1/27/2021 10:32 PM
Formatted: English (US)
- Naomi Ochwat 1/17/2021 9:36 PM
Deleted: Schneider, T.: Water movement in the firn of Storglaciären. *J. Glaciol.* 45, 286–294, 1999.

1490 [van Pelt, W., Pohjola, V., Pettersson, R., Marchenko, S., Kohler, J., Luks, B., Hagen, J. O., Schuler, T. V., Dunse, T., Noël,](#)
1491 [B., and Reijmer, C.: A long-term dataset of climatic mass balance, snow conditions, and runoff in Svalbard \(1957–2018\),](#)
1492 [The Cryosphere, 13, 2259–2280, <https://doi.org/10.5194/tc-13-2259-2019>, 2019.](#)

1493 Wagner, P. W.: Description and evolution of snow and ice features and snow surface forms on the Kaskawulsh Glacier.
1494 Icefield Ranges Research Project: Scientific Results, 1, 51–53, 1969.

1495 [Vionnet, V., Brun, E., Morin, S., Boone, A., Faroux, S., Le Moigne, P., et al.: The detailed snowpack scheme Crocus and its](#)
1496 [implementation in SURFEX v7.2, *Geosci. Model Dev.*, 5, 773–791, doi: 10.5194/gmd-5-773-2012, 2012.](#)

1497 Williamson, S., Zdanowicz, C., Anslow, F., S. Clarke, G. K. C., Copland, L., Danby, R. K., Flowers, G. E., Holdsworth, G.,
1498 Jarosch, A. H., and Hik, D. S.: Evidence for elevation-dependent warming in the St. Elias Mountains, Yukon, Canada. *J.*
1499 *Clim.* 3253–3269, <https://doi.org/10.1175/jcli-d-19-0405.1>, 2020.

1500 Wood, W. A.: The Icefield Ranges Research Project. *Geo. Rev.* 53, 503–529. <https://doi.org/10.1126/science.15.370.195>,
1501 1963.

1502 Yalcin, K., Wake, C. P., Kreutz, K. J., and Whitlow, S. I.: A 1000-yr record of forest fire activity from Eclipse Icefield,
1503 Yukon, Canada. *The Holocene*, 16(2), 200–209, <https://doi.org/10.1191/0959683606hl920rp>, 2006.

1504 Young, E. M., Flowers, G. E., Berthier, E. and Latto, R.: An imbalancing act: the [delayed](#) dynamic response of the
1505 Kaskawulsh Glacier to [sustained mass loss](#), *Journal of Glaciology*, 18 pp, <https://doi.org/10.1017/jog.2020.107>, 2020.

1506 [Zagorodnov, V., Nagornov, O., and Thompson, L.: Influence of air temperature on a glacier’s active-layer temperature,](#)
1507 [Annals of Glaciology, 43, 285–291. doi:10.3189/172756406781812203, 2006.](#)

1508 Zdanowicz, C., Smetny-Sowa, A., Fisher, D., Schaffer, N., Copland, L., Eley, J., and Dupont, F.: Summer melt rates on
1509 Penny Ice Cap, Baffin Island: Past and recent trends and implications for regional climate, *J. Geophys. Res. Earth Surf.* 117,
1510 F02006, <https://doi.org/10.1029/2011JF002248>, 2012.

1511 Zdanowicz, C., Fisher, D., Bourgeois, J., Demuth, M., Sheng, J., Mayewski, P., Kreutz, K., Osterberg, E., Yalcin, K., Wake,
1512 C., Steig, E., Froese, D., and Goto-Azuma, K.: Ice [cores](#) from the St. Elias Mountains, Yukon, Canada: Their [significance](#) for
1513 [climate, atmospheric composition and volcanism in the North Pacific region](#), *Arctic*, 1–23, 2014.

1514

Shawn Marshall 1/16/2021 12:36 PM
Formatted ... [57]

Naomi Ochwat 1/28/2021 7:30 PM
Formatted ... [58]

Shawn Marshall 1/16/2021 12:36 PM
Formatted ... [59]

Shawn Marshall 1/16/2021 1:08 PM
Deleted: a changing mass budget... ustaine ... [60]

Shawn Marshall 1/20/2021 9:22 AM
Formatted: Font:(Default) +Theme

Naomi Ochwat 1/28/2021 7:30 PM
Formatted ... [61]

Shawn Marshall 1/16/2021 1:07 PM
Deleted: .

Shawn Marshall 1/20/2021 9:22 AM
Formatted: Font:(Default) +Theme

Shawn Marshall 1/16/2021 12:38 PM
Deleted: .

Naomi Ochwat 1/28/2021 10:19 PM
Formatted: Space After: 12 pt, Line spacing: single

Shawn Marshall 1/16/2021 12:38 PM
Deleted: Cores ...ores from the St. Elias ... [62]

1534

1535

1536 **Table 1:** Total ice content, ice fraction (F_i), bulk density (ρ_b) and background density (ρ_f), for the firm portion of each core.

1537 Depths are reported from the May 2018 snow surface, and the firm portion of the core started at the 2017 summer surface, at
1538 4.2 m depth.

1539

	Depth below surface (m)	Total Ice content (m)	F_i (% vol)	F_i (% mass)	ρ_b (kg m ⁻³)	ρ_f (kg m ⁻³)	w w.e. (m)
Core 1	4.2-14.2	0.67 ± 0.07	6.7 ± 0.7	13.0 ± 1.3	588 ± 8	565 ± 9	5.88 ± 0.08
	4.2-21.6	1.51 ± 0.15	8.7 ± 0.9	15.6 ± 1.6	640 ± 6	613 ± 7	11.08 ± 0.11
	4.2-36.6	2.33 ± 0.26	7.2 ± 0.7	11.9 ± 1.2	698 ± 5	676 ± 6	22.49 ± 0.15
Core 2	4.2-14.2	0.42 ± 0.04	4.2 ± 0.4	8.4 ± 0.8	572 ± 7	556 ± 7	5.72 ± 0.07
	4.2-21.6	0.81 ± 0.08	4.7 ± 0.5	8.5 ± 0.9	624 ± 5	609 ± 6	10.85 ± 0.09
Average	4.2-14.2	1.18	4.0	564	580 ± 5	560 ± 5	5.80 ± 0.05
	4.2-21.6				632 ± 4	611 ± 4	10.97 ± 0.07

1540

1541

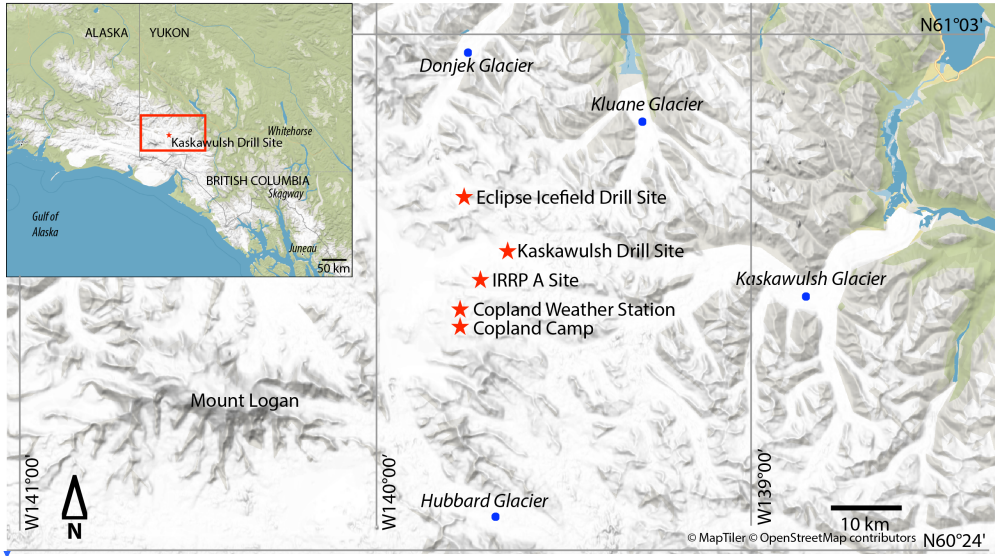
- Shawn Marshall 12/28/2020 6:12 PM
Deleted: 2018
- Shawn Marshall 12/28/2020 6:12 PM
Deleted: seasonal
- Shawn Marshall 12/28/2020 6:12 PM
Deleted: ;
- Shawn Marshall 12/28/2020 6:11 PM
Deleted: below
- Shawn Marshall 12/28/2020 6:11 PM
Deleted: last

1547
 1548
 1549 **Table 2:** Climate, surface energy balance, and firn conditions, 1965 to 2019, based on the ERA meteorological forcing at the
 1550 core site. Decadal trends are reported from linear fits to the data. The period 1965-1975 represents the historical baseline
 1551 period, when much of the work of the IRRP was completed. 2005-2017 represents the period of record of Core 1, and 2013
 1552 was an exceptional year which potentially marked the initial development of the firn aquifer at this site. [Melt and refreeze](#)
 1553 [refer to the total annual melting and refreezing in the 35-m snow and firn column, ‘drainage’ is the total annual melt minus](#)
 1554 [refreezing, and ‘net melt’ refers to the net surface melting minus refreezing, accounting for meltwater freeze-thaw cycles.](#)
 1555 [This is the actual surface drawdown associated with summer melting.](#)
 1556

	1965-2019	Trend	1965-1975	2005-2017	2013
	Mean ($\pm 1 \sigma$)	(decade ⁻¹)	Mean ($\pm 1 \sigma$)	Mean ($\pm 1 \sigma$)	
Meteorological Conditions					
T_{ann} (°C)	-10.7 ± 0.9	+0.16	-11.2 ± 0.7	-10.4 ± 1.0	-9.6
T_{JJA} (°C)	-2.4 ± 0.8	+0.07	-2.2 ± 0.9	-2.1 ± 0.7	-0.7
T_{SJA} (°C)	-2.3 ± 0.8	+0.29	-2.9 ± 0.9	-1.8 ± 0.6	-0.8
PDD (°C d)	54 ± 23	+3.6	49 ± 16	69 ± 31	123
q_v (g kg ⁻¹)	3.7 ± 0.2	+0.10	3.5 ± 0.2	3.9 ± 0.2	4.2
Surface Energy Balance (JJA values)					
Q^* (W m ⁻²)	18 ± 11	+3.7	8 ± 3	26 ± 13	45
Q_N (W m ⁻²)	10 ± 9	+2.6	4 ± 3	16 ± 13	37
net melt (mm w.e. yr ⁻¹)	230 ± 210	+62	100 ± 80	380 ± 310	895
melt (mm w.e. yr ⁻¹)	520 ± 270	+81	360 ± 130	720 ± 375	1360
refreeze (mm w.e. yr ⁻¹)	500 ± 195	+48	360 ± 130	615 ± 205	1100
drainage (mm w.e. yr ⁻¹)	20 ± 120	+32	0 ± 0	105 ± 215	260
Firn Conditions					
T_1 (°C)	-12.8 ± 0.9	+0.2	-13.3 ± 0.8	-12.4 ± 0.9	-11.5
T_{10} (°C)	-7.3 ± 3.4	+1.8	-11.3 ± 0.8	-2.9 ± 2.4	-3.0
T_{20} (°C)	-7.2 ± 3.6	+2.1	-12.2 ± 0.5	-3.7 ± 2.5	-4.5
T_{35} (°C)	-8.0 ± 3.5	+2.1	-12.7 ± 0.4	-4.8 ± 1.9	-5.2
\bar{r}_{thaw} (m)	6.8 ± 9.4	+3.6	1.2 ± 1.0	13.1 ± 12.5	18.0
E_{lat} (MJ m ⁻²)	126 ± 41	+9.3	98 ± 30	147 ± 43	258
ρ_g (kg m ⁻³)	655 ± 10	+4.6	645 ± 3	663 ± 12	671
ice content (m)	2.0 ± 0.6	+0.2	1.1 ± 0.3	2.3 ± 0.4	2.6

Formatted [63]
 Shawn Marshall 1/2/2021 10:39 AM
 Deleted: 8
 Shawn Marshall 12/28/2020 10:25 AM
 Formatted [64]
 Shawn Marshall 12/28/2020 10:25 AM
 Formatted [65]
 Shawn Marshall 1/2/2021 11:47 AM
 Deleted: 0
 Shawn Marshall 1/2/2021 11:51 AM
 Deleted: 3...8 [72]
 Shawn Marshall 1/2/2021 11:49 AM
 Deleted: 3...7 [74]
 Shawn Marshall 1/2/2021 11:48 AM
 Deleted: 1
 Shawn Marshall 1/2/2021 11:48 AM
 Deleted: 0
 Shawn Marshall 1/2/2021 11:49 AM
 Deleted: 3
 Shawn Marshall 1/19/2021 9:21 AM
 Formatted [66]
 Shawn Marshall 1/2/2021 10:47 AM
 Deleted: -
 Shawn Marshall 1/2/2021 11:47 AM
 Deleted: 3
 Shawn Marshall 1/2/2021 11:48 AM
 Deleted: 1
 Shawn Marshall 1/2/2021 11:48 AM
 Deleted: 0
 Shawn Marshall 1/2/2021 11:49 AM
 Deleted: 2
 Shawn Marshall 1/2/2021 11:49 AM
 Deleted: 8
 Shawn Marshall 1/2/2021 11:49 AM
 Deleted: 2
 Shawn Marshall 1/19/2021 9:21 AM
 Formatted [67]
 Shawn Marshall 1/19/2021 9:21 AM
 Formatted [68]
 Shawn Marshall 1/20/2021 9:22 AM
 Formatted [69]
 Shawn Marshall 1/20/2021 9:22 AM
 Formatted [70]
 Shawn Marshall 1/2/2021 12:00 PM
 Formatted [71]
 Shawn Marshall 1/2/2021 12:00 PM
 Formatted [73]
 Shawn Marshall 1/2/2021 12:00 PM
 Formatted [75]
 Shawn Marshall 1/2/2021 12:00 PM
 Formatted [76]
 Shawn Marshall 1/2/2021 12:00 PM
 Formatted [77]
 Shawn Marshall 1/2/2021 12:00 PM
 Formatted [78]
 Shawn Marshall 1/2/2021 12:00 PM
 Formatted [79]
 Shawn Marshall 1/2/2021 12:00 PM
 Formatted [80]
 Shawn Marshall 1/2/2021 12:00 PM
 Formatted [81]
 Shawn Marshall 1/2/2021 10:36 AM
 [82]
 Shawn Marshall 1/20/2021 9:22 AM
 Formatted [83]
 Shawn Marshall 1/2/2021 10:39 AM
 [84]
 Shawn Marshall 1/20/2021 9:22 AM
 Formatted [85]
 Shawn Marshall 1/2/2021 10:42 AM
 Formatted [86]
 Shawn Marshall 1/2/2021 12:02 PM
 [87]
 Shawn Marshall 1/2/2021 10:36 AM
 [88]
 Shawn Marshall 1/20/2021 9:21 AM

1745



1746

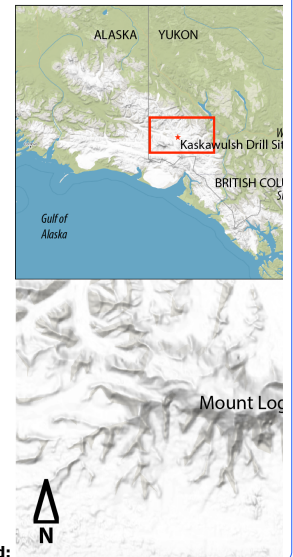
1747

1748

1749

Figure 1: Field locations in the St. Elias Icefield, Yukon. IRRP A site is the site of the 1964 firn core that is referenced in our study (Grew and Mellor, 1966). Base map from <http://openmaptiles.org/>.

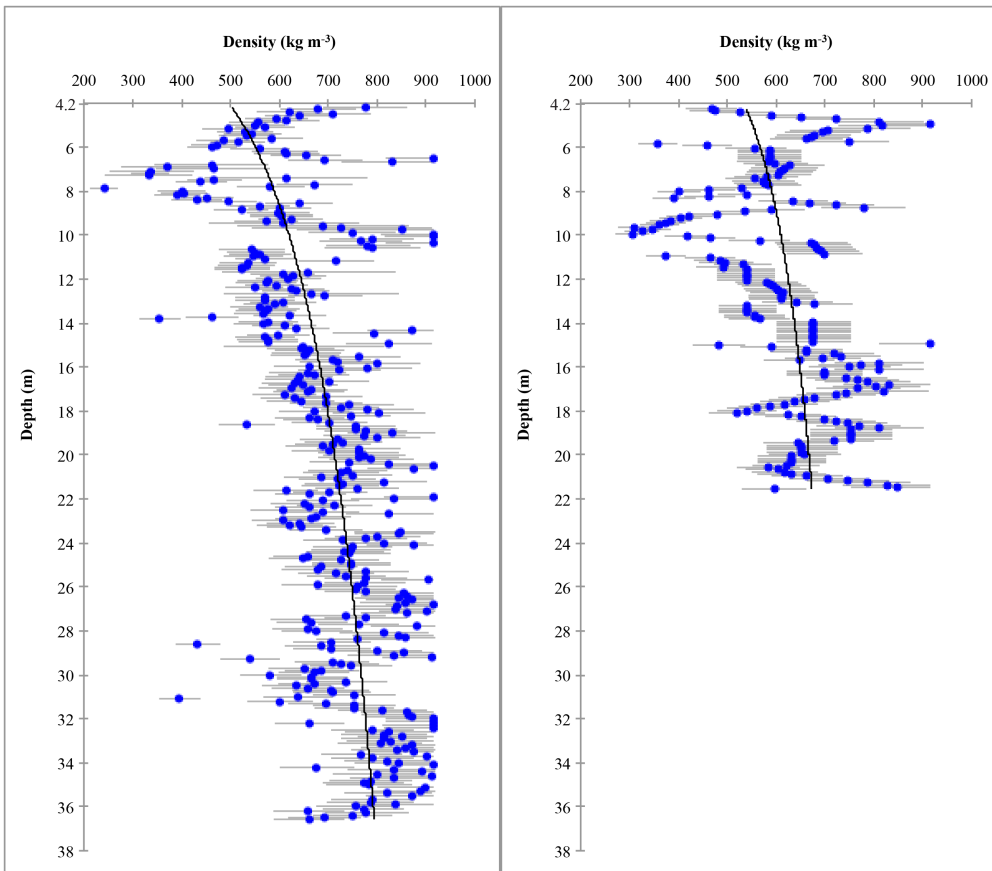
Alison Criscitiello 1/25/2021 4:44 PM



Deleted:

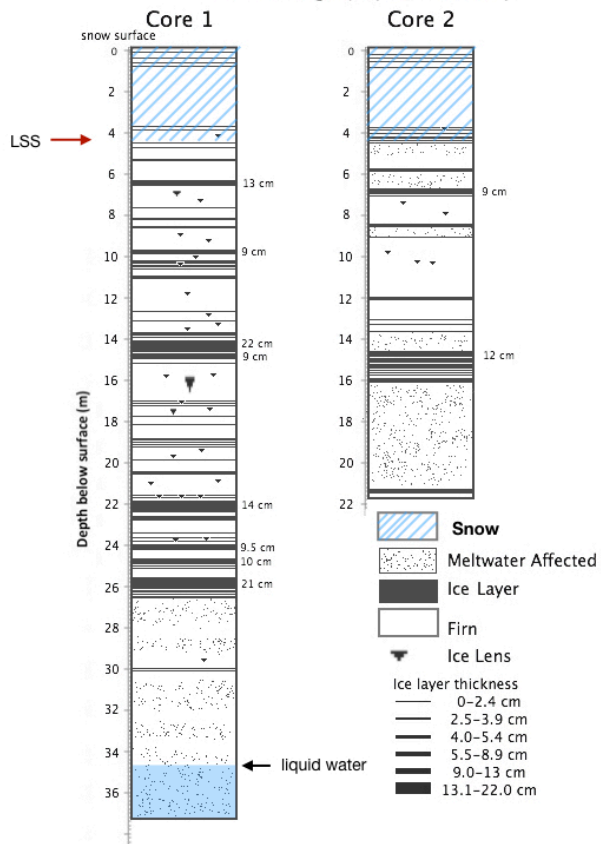
Shawn Marshall 1/7/2021 9:51 AM

Deleted: divide site referenced in the IRRP



1752
 1753 **Figure 2:** Measured firn densities of: (A) Core 1, and (B) Core 2 (May 20-24th 2018), with uncertainties and best-fit
 1754 logarithmic curves (black line). The depth scales are truncated at the location of the last summer surface at 4.2 m depth, as
 1755 the profile consisted of seasonal snow above this.

Firn Stratigraphy and Density



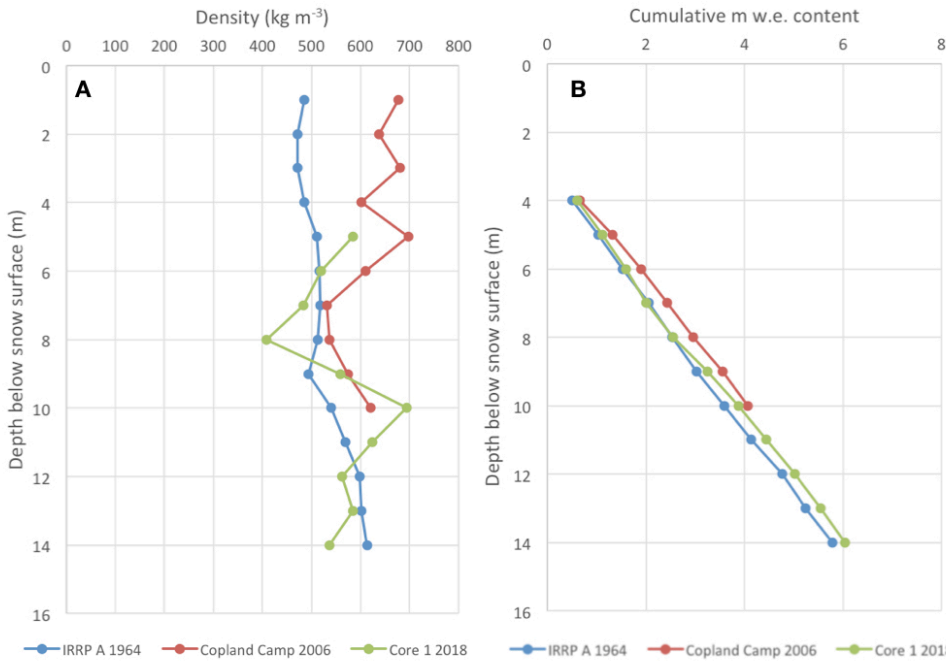
1756

1757 **Figure 3:** Stratigraphy of the cores collected in May 2018. LSS is the last summer surface, the boundary between seasonal
 1758 snow above and firn below. Ice layer thicknesses were classified in the legend by thickness distribution. Note that the ice
 1759 layers in the first several meters of the core are interpreted as wind crusts.

1760

1761

1762



1764

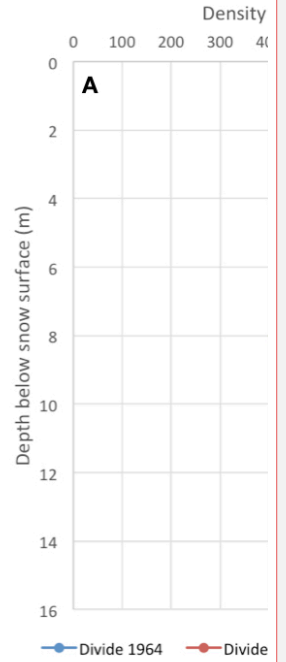
1765

1766 **Figure 4:** A) Comparison of densities averaged over 1 m segments at [JRRP A](#) on July 23, 1964 (Grew and Mellor, 1966;
 1767 blue); at [Copland Camp](#) on July 14-17, 2006 (red); at [Core 1](#) on May 20-24, 2018 (green). Depth of LSS (i.e., boundary
 1768 between seasonal snow above and firn below) was 3.28 m in 1964, 3.50 m in 2006, and 4.22 m in 2018; the density data for
 1769 2018 begins at the LSS due to the difference in time of year of the measurements compared to the others; B) Comparison
 1770 between cumulative w.e. content in the 1964, 2006 and 2018 profiles, starting at the LSS.

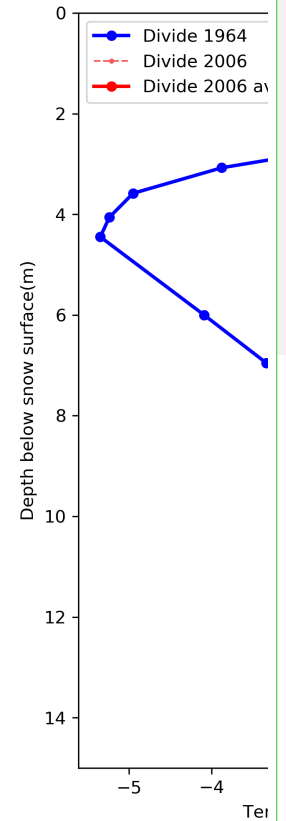
1771

1772

1773

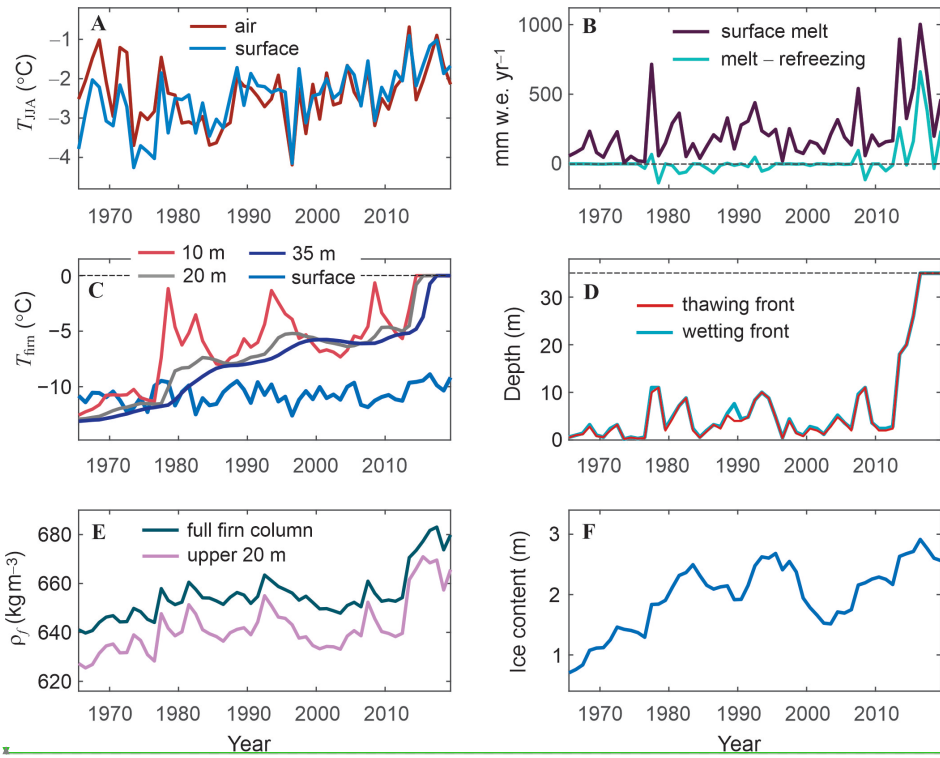


Deleted:
 Luke Copland 1/25/2021 2:45 PM
 Deleted: Divide ...RRP A on July 23, 19... [109]
 Alison Criscitiello 1/25/2021 8:30 PM
 Deleted: c
 Shawn Marshall 1/3/2021 4:20 PM



Deleted:
 Shawn Marshall 1/3/2021 4:20 PM

1795
1796
1797



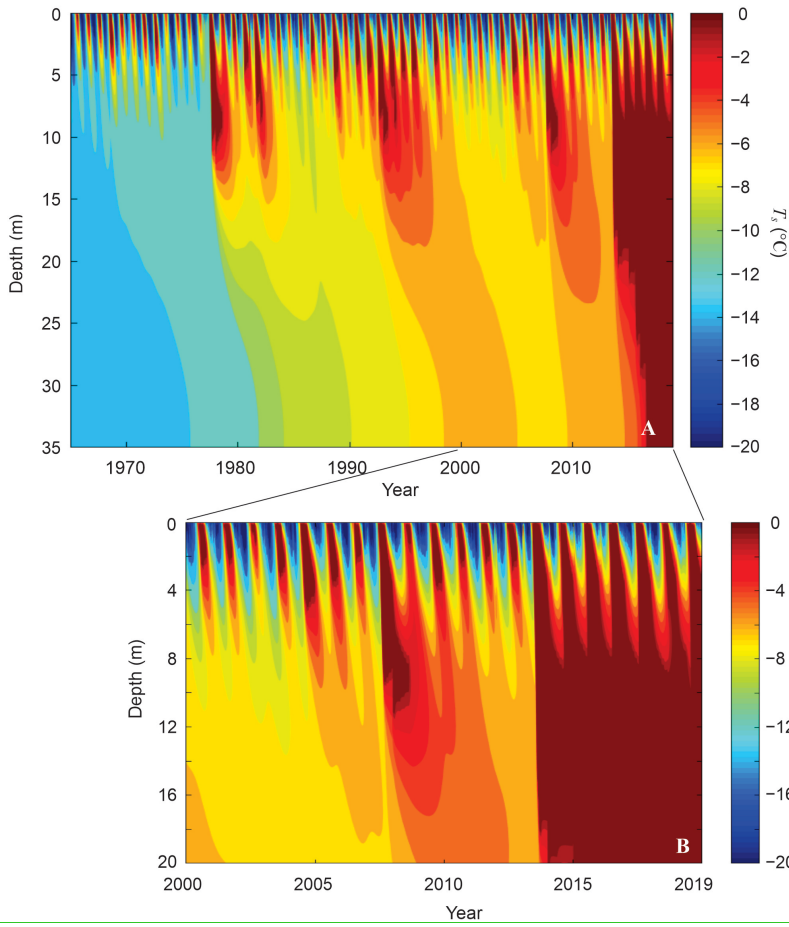
1798
1799

1800 **Figure 5:** Modelled meteorological, surface mass balance, and firn conditions from 1965 to 2019: (A) Summer (JJA) air and
1801 snow-surface temperatures, °C; (B) Annual melting and drainage (melting minus refreezing), mm w.e. yr⁻¹; (C) Annual
1802 mean snow and firn temperature at the surface (0.1 m) and at depths of 10, 20, and 35 m, °C; (D) Modelled maximum depths
1803 of the summer wetting and thawing fronts, m; (E) Average firn density for the full firn column and in the upper 20 m, kg m⁻³;
1804 (F) total firn ice content, m.
1805

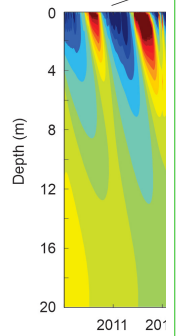
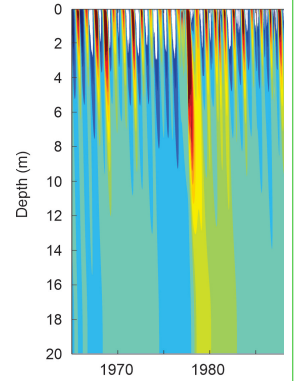
Shawn Marshall 1/3/2021 4:20 PM

Panel A: Summer (JJA) air and snow-surface temperatures in °C. Panel C: Annual mean snow and firn temperature at the surface (0.1 m) and at depths of 10, 20, and 35 m in °C.

Deleted:
Unknown
Formatted: Font:(Default) +Theme
Headings, 4 pt, Bold
Shawn Marshall 1/3/2021 4:21 PM
Deleted: 6...: Modelled meteorological, ... [110]
Shawn Marshall 1/16/2021 1:11 PM
Formatted ... [111]



Shawn Marshall 1/3/2021 4:24 PM



1816

1817

1818

1819

1820

1821

Figure 6: Modelled subsurface temperature evolution for the reference model climatology and parameter settings. (A) 1965-2019, full 35-m firn column; (B) 2000-2019, upper 20 m. Deep temperate conditions conducive to a firn aquifer developed from 2013 to 2017, in response to several subsequent summers of high melting and deep meltwater infiltration.

Deleted:

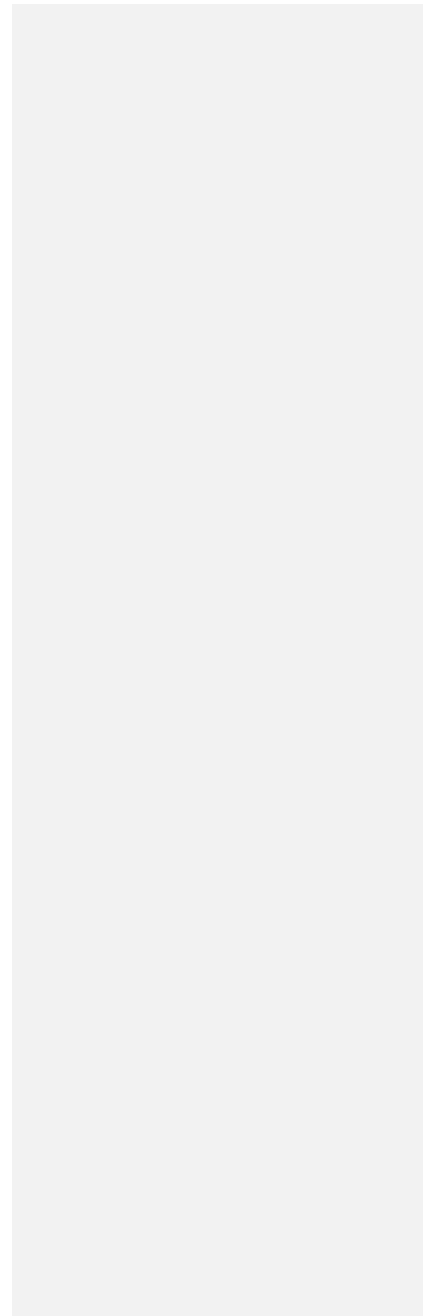
Unknown

Formatted: Font:(Default) +Theme Body,

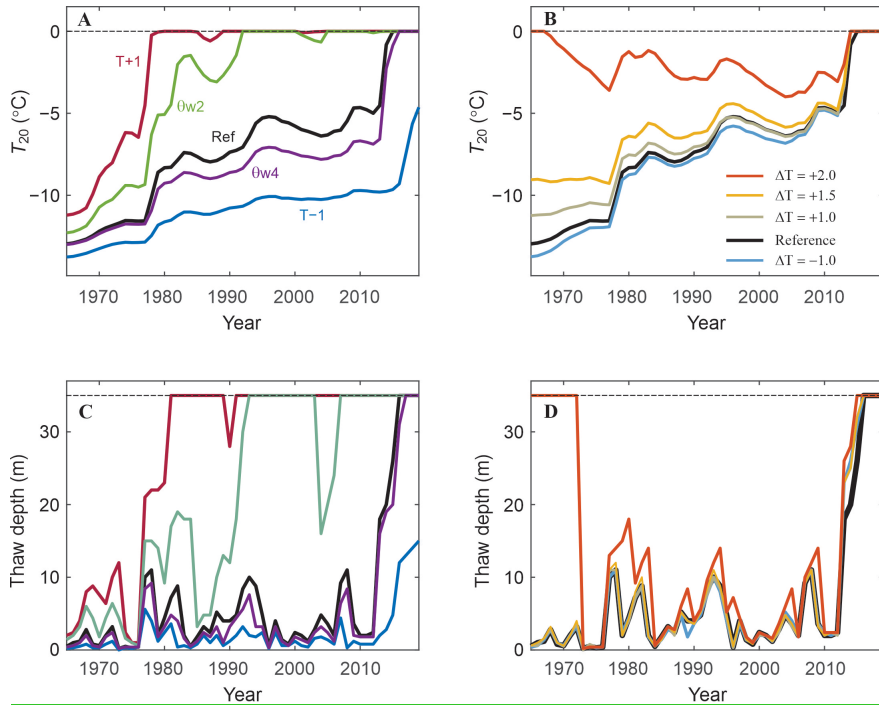
Shawn Marshall 1/3/2021 6:24 PM

Deleted: -

... [112]



1835
1836
1837
1838



1839
1840
1841
1842
1843
1844
1845
1846
1847
1848
1849

Figure 7: Sensitivity of the model simulations to (A,C) meteorological forcing and firn model parameters, and (B,D) initial conditions, through different model spin-up settings. (A) Mean annual 20-m temperatures and (C) seasonal thaw depths from 1965-2019 for the reference model and for sensitivity experiments with $\pm 1^\circ\text{C}$ and for irreducible water contents of 0.02 (θ_{w2}) and 0.04 (θ_{w4}). The line colours in (A) also apply to (C). An extended set of sensitivity tests is presented in the supplementary material. (B) 20-m temperatures and (D) thaw depths from 1965-2019 after a 30-year spin-up with perpetual 1965 climatology (the reference model) and imposed temperature anomalies of 1, 1.5, 2, and 2.5°C for the spin-up. The colour legend for (B) and (D) is indicated in (B).

Shawn Marshall 1/3/2021 6:24 PM
Deleted:

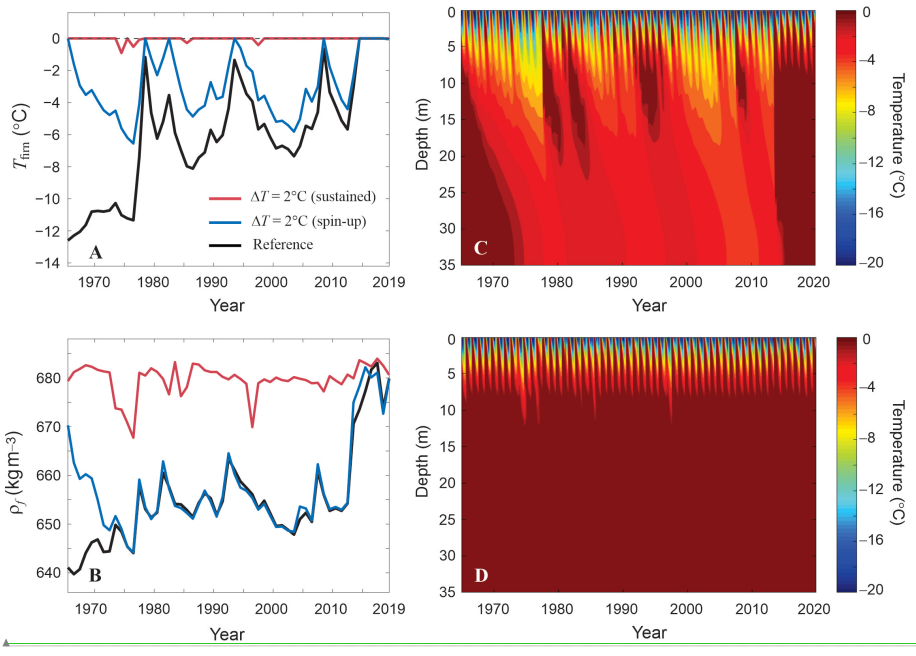
Shawn Marshall 1/3/2021 6:24 PM
Formatted: Left, Line spacing: single

Shawn Marshall 1/3/2021 4:39 PM
Formatted: Font:(Default) +Theme Headings

Shawn Marshall 1/3/2021 4:39 PM
Formatted: Font:(Default) +Theme Headings

Shawn Marshall 1/3/2021 4:39 PM
Formatted: Font:(Default) +Theme Headings

1851



1852

1853

1854

1855

1856

1857

Figure 8: Modelled (A) 10-m firn temperature and (B) average firn density for the reference model, for a 2°C temperature anomaly for the spin-up, and for a sustained temperature anomaly of +2°C. (C,D) Firn temperature evolution for (C) the warm spin-up, followed by the reference climatology, and (D) sustained 2°C temperature anomalies.

Unknown
Formatted: Font:(Default) +Theme
 Headings, Bold

Shawn Marshall 1/3/2021 4:41 PM
Formatted: Left